Two-level states in glasses

1987 Rep. Prog. Phys. 50 1657

(http://iopscience.iop.org/0034-4885/50/12/003)

Rep. Prog. Phys. **50** (1987) 1657-1708. Printed in the UK

Two-level states in glasses

W A Phillips

Cavendish Laboratory, University of Cambridge, Madingley Road, Cambridge CB3 0HE, UK

Abstract

This review covers a wide range of experimental and theoretical studies of two-level or tunnelling states in glasses. Emphasis is on fundamental physics rather than a detailed comparison of experiment and theory. Sections cover the static and dynamic properties of tunnelling states, their contribution to thermal properties and their response to weak and strong electric and acoustic fields, both steady state and pulsed. A section on metallic glasses focuses on the importance of electron tunnelling-state interactions, and a final section illustrates approaches to a microscopic description by means of selected examples.

This review was received in February 1987.

0034-4885/87/121657+52$09.00

Contents

	Page
1. Introduction	1659
2. Tunnelling states	1663
2.1. Static description	1663
2.2. Dynamics	1666
3. Thermal properties	1669
3.1. Thermal conductivity	1669
3.2. Heat capacity	1670
3.3. Thermal expansion	1673
3.4. Energy relaxation and irreversibility	1675
4. Response to external fields	1677
4.1. Weak fields	1677
4.2. Strong fields	1679
4.3. Relaxation	1682
5. Pulse echo experiments	1686
5.1. General theory	1686
5.2. Echo experiments	1687
5.3. Spectral diffusion	1691
6. Metallic glasses	1696
7. Microscopic descriptions of tunnelling states	1700
7.1. Relation to specific defects	1700
7.2. Microscopic modelling	1702
7.3. General theories	1704
7.4. Suffix	1705
Acknowledgments	1706
References	1706

1. Introduction

One of the more unexpected results in solid state physics was provided by the first reliable measurements below 1 K of heat capacity C and thermal conductivity κ in a number of glasses (Zeller and Pohl 1971). Beforehand it had been argued that because low-temperature thermal properties are dominated by phonons (quantised lattice vibrations) of low frequency, and because in crystals these phonons can be described as long-wavelength sound waves propagating through an elastic continuum, there should be little difference between glasses and crystals in this regime where the phonons are insensitive to microscopic structure. In fact, as shown in figures 1 and 2 for vitreous and crystalline silica, the heat capacity and thermal conductivity are radically different in the two materials.

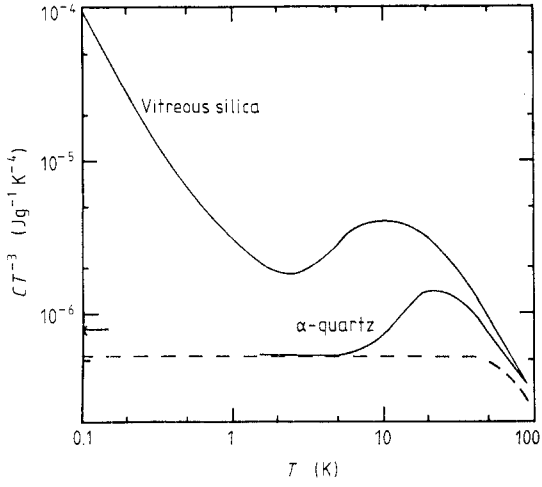

Figure 1. The heat capacity $C(T)$ of vitreous silica and crystalline quartz as a function of temperature T (Jones 1982, after Zeller and Pohl 1971), plotted as C/T^3 against T.

The results in α-quartz are typical of an insulating crystal. The heat capacity varies as T^3 below 10 K, where T is the absolute temperature, as expected from the Debye theory. This theory predicts that in the long-wavelength limit the density of phonon states $g(\omega)$ varies quadratically with the phonon (angular) frequency ω if the velocity of sound v_s is constant so that $\omega q = v_s$, where q is the phonon wavevector. At higher temperatures phonon dispersion initially gives a more rapid increase of $g(\omega)$ with ω, and so C increases more rapidly than T^3, but ultimately, above the Debye temperature θ, C approaches the classical limit.

The cubic temperature variation of κ can be interpreted qualitatively by means of the kinetic formula

$$\kappa = \tfrac{1}{3} C v_s l \tag{1.1}$$

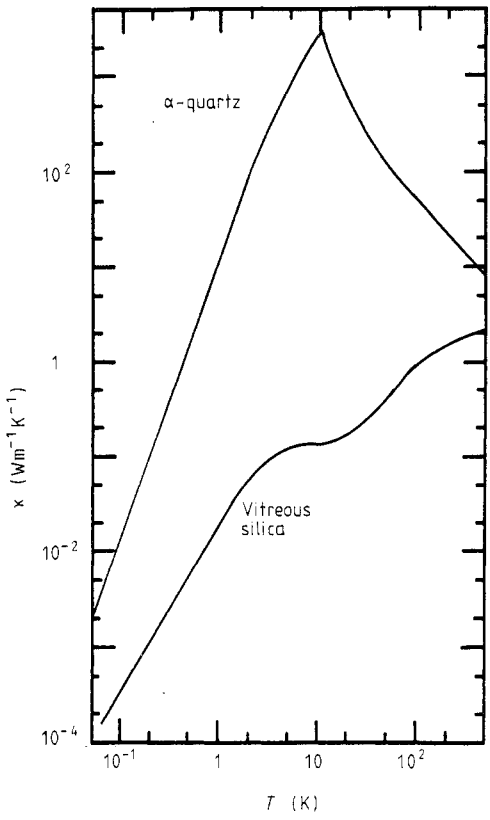

Figure 2. The thermal conductivity $\kappa(T)$ of vitreous silica and crystalline quartz (Jones 1982, after Zeller and Pohl 1971), plotted logarithmically.

where l is the phonon mean free path. At low temperatures phonons are scattered by defects in the crystal or by the surfaces of the sample, so that l is independent of temperature and κ is therefore proportional to T^3. Above 40 K the reduction of l by phonon–phonon scattering leads to the peak and subsequent fall in κ.

These ideas are well known and serve to emphasise the peculiarity of the results in vitreous silica, where C varies approximately as T and at 0.1 K is about two orders of magnitude greater in the glass than in the crystal. Below 1 K κ varies as $T^{1.9}$ but varies only slightly with temperature between 4 and 20 K before increasing at high temperatures to a value approaching that of crystalline quartz. Similar results are seen in a wide range of other amorphous solids; oxide, chalcogenide, elemental, polymeric and metallic glasses all show the same behaviour. A representative sample is shown in figures 3 and 4.

The universality of the phenomena and the idealised temperature dependences of C proportional to T and κ proportional to T^2 proved great attractions for theorists. In retrospect this idealisation can be seen to have handicapped the search for a theoretical explanation, suggesting as it did very general models which were not supported by a detailed examination of the experimental results and which were ultimately unable to give quantitative agreement with experiment. For example, the first and perhaps most obvious explanation for C was in terms of electron states (Redfield 1971). In the amorphous state the sharp distinction between energy gaps

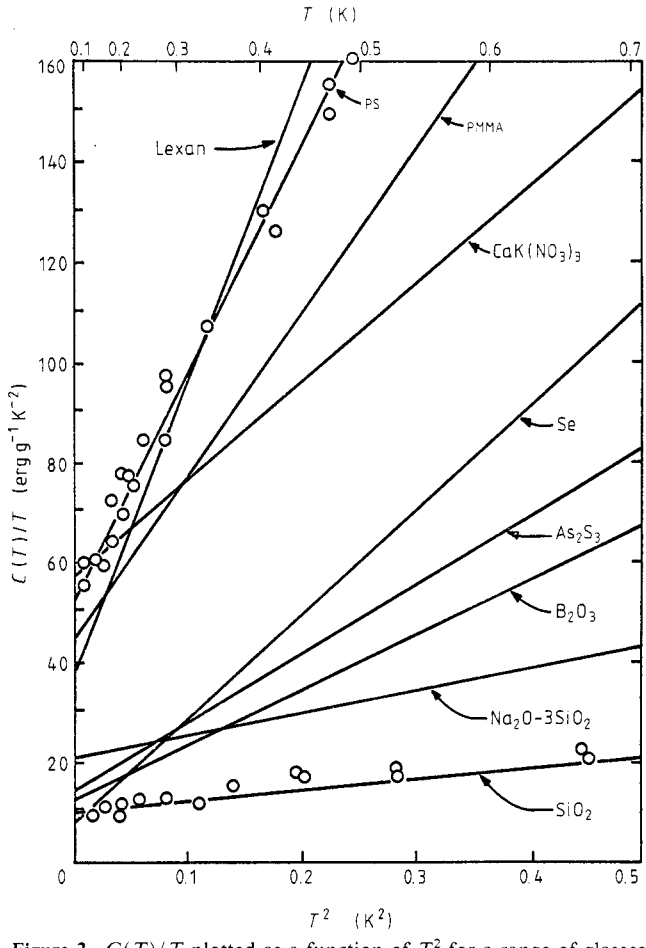

Figure 3. $C(T)/T$ plotted as a function of T^2 for a range of glasses (Stephens 1973).

and energy bands can be blurred by disorder, and it was suggested that the specific heat was a result of an almost constant density of states at the Fermi level, giving a linear variation of C with T just as in a metal. However, it turns out that the density of states estimated from optical experiments (less than 10^{43} J^{-1} m^{-3} or 10^{18} eV^{-1} cm^{-3}) is much smaller than that deduced from the heat capacity (10^{46} J^{-1} m^{-3}).

Similar quantitative problems arise in a model for thermal conductivity based on the scattering of sound waves by inhomogeneities in the glass structure, a form of Rayleigh scattering by variations in the local velocity of sound. In this case the magnitude of density fluctuations estimated thermodynamically or from light scattering experiments is too small to give significant scattering below 1 K, and although there is no independent way of directly estimating the local variation in velocity, the required magnitude is unreasonably large (Jones *et al* 1978).

Sound waves are known to exist in glasses. In addition to measurements of the velocity of sound, limited to frequencies below about 1 GHz, evidence for the existence of well defined transverse and longitudinal waves comes from Brillouin scattering below 30 GHz (Vacher and Pelous 1976) and phonon interference experiments (Rothenfusser *et al* 1983) up to 500 GHz in vitreous silica. Consistent velocities are

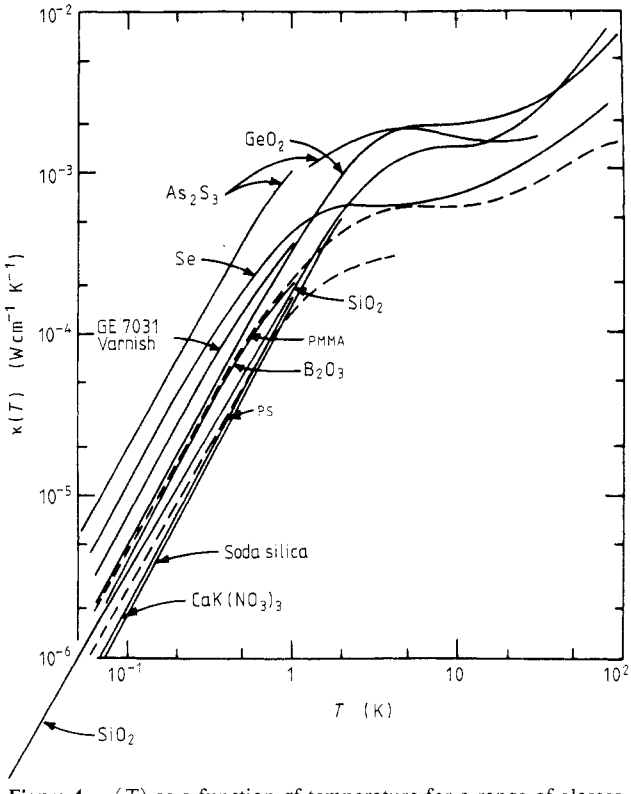

Figure 4. $\kappa(T)$ as a function of temperature for a range of glasses (Stephens 1973).

measured in all these experiments, and the phonon mean free path is much greater than the wavelength. Further evidence is provided by measurements of thermal conductivity in very thin glass rods which have roughened surfaces to ensure that boundary scattering dominates (Pohl *et al* 1974, Zaitlin and Anderson 1975). Experimental values agree with those calculated assuming the existence of sound waves. It is clear, therefore, that the unexpected thermal properties arise from additional excitations which both scatter phonons and contribute to the heat capacity.

Of the various models originally proposed to account for the thermal data, the one most widely and successfully used has been the tunnelling or two-level-system model (Phillips 1972, Anderson *et al* 1972). In this model, to be described in detail in the next section, atoms occupying one of two adjacent minima are assumed to tunnel quantum mechanically to the other, leading to a splitting of the ground state as in the ammonia molecule. The inevitable variations in local environment present in the amorphous solid give rise to a distribution of these splittings which is almost constant in energy, and hence to a heat capacity which can be evaluated as

$$C(T) = \int_0^\infty n_0 (E^2/4k_B T^2)\,\mathrm{sech}^2(E/2k_B T)\,\mathrm{d}E \tag{1.2}$$

where n_0 is the constant density of states and the other factor in the integrand is the contribution of a single two-level state (Schottky anomaly). Evaluating the integral gives

$$C(T) = (\pi^2/6) n_0 k_B{}^2 T \tag{1.3}$$

in broad agreement with experiment. These states scatter phonons, leading to a thermal conductivity proportional to T^2 and to an acoustic attenuation which can be saturated at high acoustic intensities. It is this last property that provides the strongest evidence for the model which will form the basis for the interpretation of the wide range of experimental results discussed in this review. To a large extent the model can be used in phenomenological form, and possible microscopic representations will be described only in the last section.

This review is not intended as a detailed evaluation and comparison of experimental results in specific glasses, but as a critical description of the way in which the tunnelling or two-level-system model can be used to explain a wide range of data. By far the largest number of experiments have been performed on vitreous silica, and this material will be used as a 'running example', although reference will be made to other materials when necessary.

2. Tunnelling states

2.1. Static description

In a perfect crystal each atom is constrained by symmetry to occupy a single potential minimum. Many defects, however, can be represented microscopically as interstitial or substitutional impurity atoms or molecules moving in a multi-minima potential provided by the neighbours. Such states have been extensively studied in, for example, alkali halides (Narayanamurti and Pohl 1970). At low temperatures a quantum mechanical description is necessary, and tunnelling of the atom from one minimum to another gives rise to the very small energy splittings (less than 10^{-4} eV) needed if the states are to be observed in thermal experiments at 1 K and below.

The tunnelling model proposes that similar states are intrinsic to glasses: an atom or group of atoms can occupy one of two (or more) potential minima. This choice at the microscopic level is consistent with the experimentally determined excess entropy of the glass with respect to the crystal, although the number of atoms contributing at low temperatures is only a small fraction of the total. The remainder are essentially immobile below the glass-transition temperature T_g.

Each tunnelling state (TS) can be represented by a particle in a potential of the form shown in figure 5(a), where the abscissa may represent the position of one atom but more generally is a configurational coordinate describing a combination of the coordinates of a number of atoms. The energy levels of the particle are conveniently calculated using as a starting point the solutions of the single-well problem, a choice of basis set ϕ_1 and ϕ_2 known as the *well, non-diagonal* or *localised* representation (figure 5(b)). Each state is the ground state of the appropriate potential V_1 or V_2 (assumed harmonic in figure 5). The complete Hamiltonian H can be written as

$$H = H_1 + (V - V_1) = H_2 + (V - V_2) \tag{2.1}$$

where H_1 and H_2 are the individual well Hamiltonians. In the localised representation the Hamiltonian matrix becomes

$$\begin{vmatrix} E_1 + \langle \phi_1 | V - V_1 | \phi_1 \rangle & \langle \phi_1 | H | \phi_2 \rangle \\ \langle \phi_2 | H | \phi_1 \rangle & E_2 + \langle \phi_2 | V - V_2 | \phi_2 \rangle \end{vmatrix}. \tag{2.2}$$

If the extension of each localised wavefunction into the barrier is small, the terms $\langle \phi_i | V - V_i | \phi_i \rangle$ can be neglected in comparison to E_i, and if the zero of energy is chosen

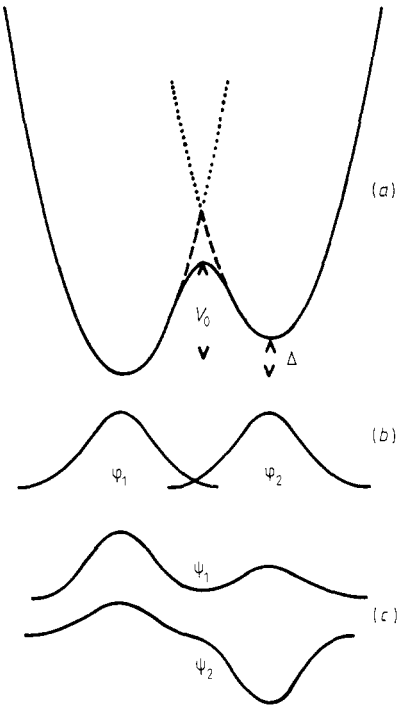

Figure 5. A double-well potential (*a*), together with the wavefunctions in the localised (*b*) and diagonal (*c*) representations.

as the mean of E_1 and E_2, (2.2) becomes

$$\tfrac{1}{2}\begin{vmatrix} -\Delta & \Delta_0 \\ \Delta_0 & +\Delta \end{vmatrix} \tag{2.3}$$

where the tunnel splitting Δ_0 is given by

$$\Delta_0 = 2\langle \phi_1 | H | \phi_2 \rangle. \tag{2.4}$$

Notice that only if the wells are identical, apart from a relative shift in energy, is the Δ of (2.3) identical to that of figure 5(a).

Δ_0 can be evaluated for specific potentials: two overlapping harmonic potentials in two and three dimensions (Mertzbacker 1970, Phillips 1981b) and Mathieu's equation for a rigid rotator in two-fold and three-fold potentials (Isnard and Gilchrist 1981) are typical examples. The results all imply a similar exponential dependence of Δ_0 on the barrier height and well separation, although precise numerical values change from one model to another. The use of a particular detailed form cannot be justified in amorphous solids (as opposed to crystals) because the microscopic picture is uncertain, and so a simplified expression is usually adequate:

$$\Delta_0 = \hbar\Omega\, e^{-\lambda} = \hbar\Omega \exp[-d(2mV_0/\hbar^2)^{1/2}] \tag{2.5}$$

where $\hbar\Omega$ is approximately equal to $(E_1 + E_2)/2$, d is the separation and V_0 the barrier between the two wells, and m is the particle mass.

Typical values of the tunnelling parameter λ can be estimated from the requirement that Δ_0 must be approximately equal to $k_B T$ if the tunnelling state is to contribute to

thermal properties at a temperature T. At 1 K this requires a tunnel splitting of 10^{-4} eV, which with $\hbar\Omega$ equal to 10^{-2} eV gives approximately 5 for λ. This is equivalent to a bare proton tunnelling across a barrier of 0.1 eV with $d = 0.7$ Å.

The matrix (2.3) can be diagonalized to obtain the eigenstates, the *true, diagonal* or *energy* representation. These eigenfunctions, illustrated in figure 5, have energies $\pm E/2$ where

$$E^2 = (\Delta^2 + \Delta_0^2)^{1/2} \tag{2.6}$$

and can be written in the analytic forms

$$\psi_1 = \phi_1 \cos\theta + \phi_2 \sin\theta \tag{2.7}$$

$$\psi_2 = \phi_1 \sin\theta - \phi_2 \cos\theta \tag{2.8}$$

where $\tan 2\theta = \Delta_0/\Delta$. In the symmetric case where $\Delta = 0$ these equations give the expected symmetric and antisymmetric solutions.

The dipole moment of the tunnelling state can be written in terms of ψ_1 and ψ_2 as

$$\begin{aligned} p_1 &= \int \psi_1^* q x \psi_1 \, \mathrm{d}x \\ &= q \int (\phi_1^* x \phi_1 \cos^2\theta + \phi_2^* x \phi_2 \sin^2\theta + \phi_1^* x \phi_2 \sin 2\theta) \, \mathrm{d}x \\ &= p_0 \Delta / E \end{aligned} \tag{2.9}$$

if the term involving $\phi_1^* x \phi_2$ can be neglected, and where p_0 is the dipole moment when the particle is located in one well:

$$p_0 = \int \phi_1^* x \phi_1 \, \mathrm{d}x = -\int \phi_2^* x \phi_2 \, \mathrm{d}x.$$

Obviously p_1 is zero for the symmetric case.

For this, as for any problem involving two energy levels, there is a formal analogy with the problem of a spin-$\frac{1}{2}$ particle in a magnetic field. The Hamiltonian matrix (2.3) can therefore be rewritten in terms of the Pauli spin matrices

$$\sigma_x = \begin{vmatrix} 0 & 1 \\ 1 & 0 \end{vmatrix} \qquad \sigma_y = \begin{vmatrix} 0 & -\mathrm{i} \\ \mathrm{i} & 0 \end{vmatrix} \qquad \sigma_z = \begin{vmatrix} 1 & 0 \\ 0 & -1 \end{vmatrix} \tag{2.10}$$

(or equivalently in terms of the spin operators $S_i = \frac{1}{2}\hbar\sigma_i$). After diagonalisation, the Hamiltonian takes the obvious form

$$H = \tfrac{1}{2} E \sigma_z.$$

This analogy has important advantages when discussing non-linear and coherent effects in the interaction of tunnelling states with acoustic and electric fields (§ 5).

A basic feature of the tunnelling state model as applied to amorphous solids is the existence of a wide range of values of both the tunnelling parameter λ and the asymmetry Δ. Calculated properties of the states will depend critically on the form of the distribution function $f(\Delta, \Delta_0)$ for Δ and Δ_0, the latter distribution derived from that for λ.

In the case of the asymmetry Δ it is argued that the distribution function must be symmetric because both positive and negative values of Δ are equally likely. (No singularities are expected for $\Delta = 0$ because the eigenstates remain non-degenerate.) The scale of energy variation is determined by the thermal energy available at the

glass-transition temperature where the fluctuating local potentials of the liquid are frozen in the structure. Since T_g is between 200 and 1000 K for most glasses, this energy is of the order of 0.05 eV, much larger than the thermal energy available at 1 K. The low temperature properties are therefore sensitive to the centre of a broad symmetric distribution, so that $f(\Delta, \Delta_0)$ can be taken as independent of Δ.

The variation with Δ_0 is likely to be sensitive to the particular microscopic motion involved, although the general form can be deduced from the distribution of the tunnelling parameter λ. Because of the exponential dependence of Δ_0 on λ, only a relatively small range of λ is sampled for a large range of Δ_0 and over this limited range the distribution of λ can be assumed constant. The resulting distribution function can then be written

$$f(\Delta, \Delta_0) = P/\Delta_0. \tag{2.11}$$

This general result is only slightly modified (by a logarithmic factor) if the distribution of λ varies slowly with the energy, but in general the precise dependence on Δ_0 will vary from one material to another, and can be regarded as a parameter to be determined by experiment (Frossatti *et al* 1977, Phillips 1981b).

The density of states $n(E)$ can be calculated from (2.6) and the distribution function $f(\Delta, \Delta_0)$ only if a lower cut-off value for Δ_0 is introduced when integrating (2.11). Such a cut-off could arise from a maximum tunnelling parameter (Lasjaunias *et al* 1978) or from characteristic time scales introduced by experiment. More precisely, the two parameters Δ and Δ_0 describing the states must be replaced by a second pair of parameters, often chosen as the energy E and the relaxation time τ. The resulting distribution function for E and τ will be derived in § 3.

In many cases the results of experiment can be interpreted and related in terms of a simpler model which ignores the detailed origin of the two levels. Instead, of two parameters Δ and Δ_0, this two-level-system model considers the total energy E as the only variable. The distribution function is assumed to be constant. Although in many cases it is clear that the two-level-system model is inadequate for detailed understanding, in others the simplification introduced by its use is very helpful.

2.2. Dynamics

The behaviour of a tunnelling state is defined by specifying the complex amplitudes $a_1(t)$ and $a_2(t)$ of the two lowest states with eigenfunctions $\psi_1(r)$ and $\psi_2(r)$. Neglect of higher states is justified because these two states are much closer in energy to each other than they are to other excited states, although the possibility that higher energy states might be important must be considered in certain cases (such as transition rates at temperatures above 1 K). The general time-dependent wavefunction takes the form

$$\Psi(r, t) = a_1(t)\psi_1(r) \exp(-iE_1 t/\hbar) + a_2(t)\psi_2(r) \exp(-iE_2 t/\hbar) \tag{2.12}$$

where E_1 and E_2 are the energies of states ψ_1 and ψ_2 and for normalisation $a_1 a_1^* + a_2 a_2^* = 1$.

The complex nature of a_1 and a_2 means that two quantities are necessary to define the two-level system, normally taken as the difference in probabilities of finding the system in the two states, $a_2 a_2^* - a_1 a_1^*$, and a quantity related to the phase difference between a_1 and a_2, $a_1 a_2^*$. Measurable properties of the system depend on these two parameters, as can be seen for example by calculating the time-dependent dipole

moment of a one-dimensional tunnelling state. Using $p_1 = -p_2 = \langle\psi_1|x|\psi_1\rangle$ and $p_{12} = p_{21} = \langle\psi_1|x|\psi_2\rangle$, the average dipole moment $\langle p(t)\rangle$ can be written

$$\langle p(t)\rangle = p_1(a_1a_1^* - a_2a_2^*) + p_{12}[a_1a_2^* \exp(i\omega_0 t) + a_2a_1^* \exp(-i\omega_0 t)] \tag{2.13}$$

where $\hbar\omega_0 = E_2 - E_1$.

Variations of $a_1(t)$ and $a_2(t)$ are determined through the time-dependent Schrödinger equation by interaction with external fields. Any two-level system in a solid will be subject to randomly varying strain fields which can be treated as the superposition of independent phonon modes. The strain field of each is weak, and interaction with the two levels can be treated using perturbation theory, ignoring phase coherence, equivalent to the interaction of an atom with electromagnetic radiation in a black-body cavity (Phillips 1981b). Experimentally the properties of the states may be probed by strong external applied electromagnetic or strain fields where coherence of the two wavefunctions ψ_1 and ψ_2 must be taken into account, although for weak external fields perturbation theory can still be used.

Two related simplifications can be made. The frequency needed to induce resonant transitions from one level to the other is less than 20 GHz for states contributing to thermal properties below 1 K. Corresponding wavelengths are 10 mm for photons and 100 nm for acoustic phonons, in both cases much larger than the spatial extent of the tunnelling or two-level state. The dipole approximation, where the local electric or strain field is taken as uniform, is therefore valid. The dominant effect of these uniform fields is to affect the energy of the tunnelling state by changing the asymmetry energy, and changes in the barrier height can usually be ignored (Phillips 1981b, Anderson 1986). Any external perturbation is therefore diagonal in the local representation (ϕ_1, ϕ_2) which when transformed into the diagonal representation (ψ_1, ψ_2) has the form

$$\begin{vmatrix} \cos 2\phi & \sin 2\phi \\ \sin 2\phi & -\cos 2\phi \end{vmatrix} \quad \text{or} \quad \begin{vmatrix} \Delta/E & \Delta_0/E \\ \Delta_0/E & -\Delta/E \end{vmatrix}. \tag{2.14}$$

In terms of the Pauli matrices the general interaction Hamiltonian can be written

$$H_{\text{int}} = \left|\frac{\Delta}{E}\sigma_z + \frac{\Delta_0}{E}\sigma_x\right| \boldsymbol{p}_0 \cdot \boldsymbol{\xi} + \left|\frac{\Delta}{E}\sigma_z + \frac{\Delta_0}{E}\sigma_x\right| \gamma e \tag{2.15}$$

in the presence of an electric field $\boldsymbol{\xi}$ and a strain field e. The two parameters p_0 and γ, defined as $\frac{1}{2}\partial\Delta/\partial\xi$ and $\frac{1}{2}\partial\Delta/\partial e$ respectively, are equivalent to the electric and elastic dipole moments of the equivalent classical problem of a charged particle moving in the double well potential. In (2.15) the vector character of $\boldsymbol{\xi}$ is preserved, but the tensorial nature of e has been ignored and γe written as an average over orientations.

For the two-level-system model (2.15) must be replaced by an equivalent form for H_{int} in which the relationship between the diagonal (σ_z) and off-diagonal (σ_x) terms is ignored. In this model (2.15) is usually written

$$H_{\text{int}} = (\tfrac{1}{2}\mu\sigma_z + \mu'\sigma_x)\xi + (\tfrac{1}{2}D\sigma_z + M\sigma_x)e. \tag{2.16}$$

In the remainder of this section the phase coherence of ψ_1 and ψ_2 will be ignored in a calculation valid for interaction with thermal phonons and weak external fields. The only relevant parameter is therefore the occupation probability $p_1 = a_1a_1^*$, with $p_1 + p_2 = 1$. Using a rate-equation approach (Golding and Graebner 1981)

$$\dot{p}_1 = -p_1\omega_{12} + p_2\omega_{21} \tag{2.17}$$

$$\dot{p}_2 = p_1\omega_{12} - p_2\omega_{12} \tag{2.18}$$

where ω_{12} is the transition probability from state 1 to state 2. In thermal equilibrium at temperature T, p_1 and p_2 are time independent, with values p_1^0 and p_2^0, so that

$$p_1^0\omega_{12} = p_2^0\omega_{21}$$

where

$$p_2^0/p_1^0 = \exp(-E/kT) = \omega_{12}/\omega_{21} \tag{2.19}$$

if E is the energy difference between the two levels. Replacing p_2 in (2.17) gives

$$\dot{p}_1 = -p_1(\omega_{12}+\omega_{21}) + \omega_{21} \tag{2.20}$$

defining a relaxation time τ, where

$$\tau^{-1} = (\omega_{12}+\omega_{21}) = \omega_{12}[1+\exp(E/kT)]. \tag{2.21}$$

This relaxation time refers to the occupation probabilities, and so governs the relaxation of the term $a_1a_1^* - a_2a_2^*$ in the expression for $\langle p\rangle$ in (2.13). To distinguish it from the relaxation time for terms of the form $a_1a_2^*$ (see § 4.2) it is often referred to as T_1, or the spin-lattice relaxation time.

The transition probability ω_{12} can be calculated for a weak strain field using time-dependent perturbation theory to give

$$\omega_{12} = \sum_\alpha \frac{2\pi}{\hbar}|\langle\psi_1|H_{\text{int}}|\psi_2\rangle|^2 g(E)n_B(E) \tag{2.22}$$

where n_B, the Bose factor, is $[\exp(E/kT)-1]^{-1}$, $g(E)$ is the phonon density of states, and the summation is over phonon polarisations α. For an acoustic wave $2e_0\cos\omega t$ the strain amplitude per phonon is given by equating the time average classical energy per unit volume to the energy of a phonon:

$$2\rho u^2\omega^2 = \hbar\omega$$

where u is the displacement amplitude and ρ is the bulk density. The strain is given by

$$e = q_\alpha u = \left(\frac{\hbar}{2\rho\omega}\right)^{1/2} q_\alpha \tag{2.23}$$

where q_α is the phonon wavevector, and the matrix element, using the term in σ_x in H_{int} (σ_z gives nothing), becomes

$$\frac{\Delta_0}{E}\gamma_\alpha\left(\frac{\hbar}{2\rho\omega}\right)^{1/2} q_\alpha. \tag{2.24}$$

The Debye density of phonon states, valid in this low-energy limit, is

$$g(E) = E^2/2\pi^2\hbar^3 v_\alpha^3 \tag{2.25}$$

per unit volume, where v_α is the sound velocity for polarisation α. Collecting together (2.21), (2.22) and (2.24) gives

$$\tau^{-1}(E) = \sum_\alpha \frac{\gamma_\alpha^2}{v_\alpha^5}\frac{E\Delta_0^2}{2\pi\rho\hbar^4}\coth(E/2k_BT). \tag{2.26}$$

In the equivalent result for the two-level system Δ_0^2 is replaced by E^2, but it should be noted that this removes the very wide range of relaxation times predicted by (2.26) through the broad distribution of Δ_0, and found experimentally (§ 3). At higher temperatures additional higher-order processes will of course contribute to relaxation, but these have not been clearly observed in glasses.

3. Thermal properties

3.1. Thermal conductivity

The interaction between TS and phonons reduces the phonon mean free path, and is the dominant scattering mechanism in glasses below 1 K. An expression for the free path, valid for weak fields (see § 4) can be obtained from the rate equations, (2.17) and (2.18), using detailed balance between energy absorbed by the TS and energy lost by the phonons. For a single TS of energy E

$$g(E)\dot{n}_{\rm ph} = \dot{p}_1. \tag{3.1}$$

Using (2.20) and (2.22) this can be written as

$$\dot{n}_{\rm ph} = \frac{-2\pi}{\hbar}|\langle\psi_1|H_{\rm int}|\psi_2\rangle|^2[n_{\rm ph}p_1 - (n_{\rm ph}+1)n_{\rm ph}p_2] \tag{3.2}$$

defining a phonon scattering rate

$$\tau_{\rm ph}^{-1} = \frac{2\pi}{\hbar}|\langle\psi_1|H_1|\psi_2\rangle|^2 \tanh(E/2k_{\rm B}T)$$

$$= \frac{\pi\gamma_\alpha^2\omega}{\rho v_\alpha^2}\frac{\Delta_0^2}{E^2}\tanh(E/k_{\rm B}T) \tag{3.3}$$

for the scattering of phonons of polarisation α by a single state with energy E and tunnel splitting Δ_0. The total scattering at energy E is obtained by integrating over Δ_0 using

$$f(\Delta, \Delta_0) = P/\Delta_0 \tag{2.11}$$

(noting that both $+\Delta$ and $-\Delta$ contribute at a given E) which gives

$$l_\alpha^{-1}(\omega) = \frac{(\pi\gamma_\alpha^2\omega)}{(\rho v_\alpha^3)}P\tanh(\hbar\omega/2k_{\rm B}T) \tag{3.4}$$

for the free path of a phonon of angular frequency ω and polarisation α.

The thermal conductivity $\kappa(T)$ is evaluated on the assumption that heat is carried by non-dispersive sound waves, consistent with the calculations leading to (2.26) and (3.4), and that scattering from TS dominates to give

$$\kappa(T) = \frac{1}{3}\sum_\alpha\int_0^\infty C_\alpha(\omega)v_\alpha l_{\rm ph}\,{\rm d}\omega \tag{3.5}$$

$$= \frac{\rho k_{\rm B}^3}{6\pi\hbar^2}\left(\sum_\alpha\frac{v_\alpha}{P\gamma_\alpha^2}\right)T^2. \tag{3.6}$$

This gives general agreement with the experimental results below 1 K both in respect of temperature dependence and magnitude, using the constant density of states derived from the heat capacity and a coupling constant γ of order 1 eV. A more precise quantitative analysis requires information from acoustic experiments to separate longitudinal and transverse polarisation contributions in (3.6), and a more careful analysis of the heat capacity. Notice, however, that the interaction with phonons is dominated by TS with small asymmetry.

Experimentally the temperature dependence is found to range from $T^{1.8}$ to $T^{1.9}$ indicating that the distribution function (2.11) is not strictly accurate. Black (1978) has pointed out that a distribution function of the form $P(\lambda) = P\,e^{-\alpha\lambda}$ leads to $\kappa(T)$ proportional to $T^{2-\alpha}$, suggesting a width to the λ distribution in the range 5–10. This is not unreasonable, but the relatively small change in temperature dependence shows the insensitivity of the calculation of $\kappa(T)$ to the detailed form of the distribution functions.

At higher temperatures the thermal conductivity passes through a 'plateau' at temperatures between 4 and 20 K which has been explained in terms of increased scattering from a quadratically increasing density of TS (Zaitlin and Anderson 1975). Although there is some evidence from high-frequency acoustic measurements that the density of states may increase at higher energies (Pelous and Vacher 1976), it is extremely difficult to identify this contribution in the presence of relaxation scattering from the TS (§ 4), higher-order phonon processes, structure scattering or even effects of phonon localisation.

3.2. Heat capacity

The energy E and relaxation time τ are more convenient parameters than Δ and Δ_0 when discussing heat capacity and other physical consequences of the distribution of tunnelling states. A distribution function (E, τ) can be related to $f(\Delta, \Delta_0)$ by the Jacobian transformation

$$g(E, \tau)\,dE\,d\tau = f(\Delta, \Delta_0)\frac{\Delta_0 E}{2\Delta\tau}\,d\Delta\,d\Delta_0. \tag{3.7}$$

This is a general result, but making use of the specific form $f(\Delta, \Delta_0) = P/\Delta_0$,

$$g(E, \tau) = -\frac{P}{2\tau(1-\tau_{\min}(E)/\tau)^{1/2}} \tag{3.8}$$

where P is the same constant that appears in l_{ph}^{-1} (3.4) and $\tau_{\min}(E)$, defined by replacing Δ_0 by E in (2.26), is the shortest relaxation time for states of energy E. The density of states is then given by integrating over all relaxation times from $\tau_{\min}$ up to a value equal to the time scale t_0 of the experiment:

$$N(E) = \frac{-P}{2}\int_{\tau_{\min}}^{t_0}\frac{d\tau}{\tau(1-\tau_{\min}/\tau)^{1/2}}$$

$$= \tfrac{1}{2}P\ln(4t_0/\tau_{\min}). \tag{3.9}$$

The heat capacity can be calculated as in (1.1) to give

$$C(t_0) = \tfrac{1}{2}P\ln(4t_0/\tau_{\min})\int_0^\infty \frac{E^2}{4k_B T^2}\operatorname{sech}^2\left(\frac{E}{2k_B T}\right)dE$$

$$= \tfrac{1}{12}\pi^2 P k_B^2 T\ln(4t_0/\tau_{\min}) \tag{3.10}$$

where the small energy variation of the logarithmic term, in the narrow range of E close to $k_B T$ which dominates the integral, has been neglected.

Equation (3.10) encapsulates the non-equilibrium (non-ergodic) nature of amorphous solids and not surprisingly has been the subject of numerous experimental

studies. Before examining the results on short time scales, it is helpful to assess the accuracy of (3.10) in respect of 'normal' measurements, where t_0 is typically 10 s.

Figure 6 shows $C(T)$ in three samples of vitreous silica, Spectrosil B (about 1200 ppm water), Suprasil (1000 ppm water) and Suprasil W (almost no water). We will concentrate here on Suprasil *W*, where $C(T)$ varies as $T^{1.3}$ in the range 25 mK $< T <$ 250 mK, and where $P = 3 \times 10^{44}$ J^{-1} m^{-3}, $\gamma_l = 1.6$ eV and $\gamma_t = 1$ eV can be deduced from $\kappa(T)$ and phonon echo experiments (§§ 3.1 and 5). The contribution of these states to C at 0.1 K can be calculated from (3.10) as 0.35 J kg^{-1} K^{-1} (taking $t_0 = 10$ s and evaluating $\tau_{\min}$ as 1 μs) in comparison to the experimental value of 0.7 J kg^{-1} K^{-1}. The logarithmic factor varies by 1.6 between 25 and 250 mK, giving a temperature variation approximately proportional to $T^{1.2}$. Bearing in mind a possible small energy dependence of P, the predicted temperature variation of C is in good agreement with experiment, although the magnitude is too small by a factor of two (Black 1978).

This discrepancy could be ascribed to experimental uncertainties in the determination of γ_l and γ_t were it not for experiments at short time scales, which provide additional evidence that the reality is more complicated than that described by a single set of TS distributed according to (3.9). Such experiments are, however, notoriously

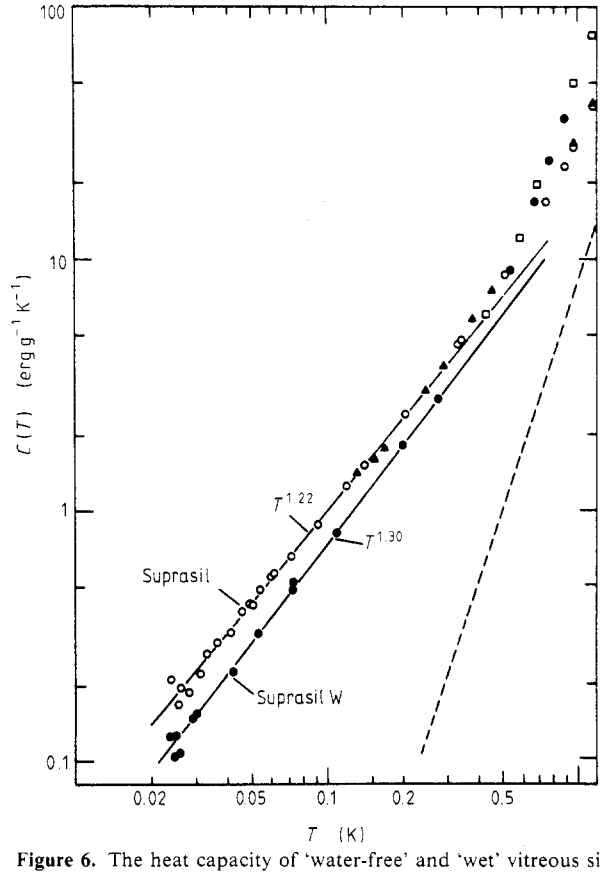

Figure 6. The heat capacity of 'water-free' and 'wet' vitreous silica down to 25 mK. Also shown as a broken line is the Debye phonon contribution calculated from the velocities of sound (Lasjaunias *et al* 1975). ●, □, Suprasil W (<1.5 ppm OH); ○, Suprasil (1200 ppm OH); ▲, Spectrosil B (~1000 ppm OH) (Zeller and Pohl 1971).

difficult (Goubau and Tait 1975, Kummer *et al* 1978, Lewis *et al* 1978, Loponen *et al* 1980, 1982, Meissner and Spitzmann 1981). In general a short time scale is achieved by using thin samples of glass; at 0.4 K a sample 0.1 mm thick has a diffusion time of typically a few μs. With a thin film heater on one side and a thermometer on the other the propagation of heat pulses through the sample can be followed to give either the diffusivity by fitting a diffusion equation to the measured temperature profile or the heat capacity by measuring the maximum temperature rise. One problem with this experimental arrangement is that even very thin metal films used as heaters or thermometers can have heat capacities comparable with the glass sample so that modelling thermal diffusion becomes difficult.

There is limited agreement between the various experiments. Although all claim to see a time-dependent heat capacity, the size of the effect differs greatly from one experiment to the next. The most consistent results are those of Meissner and Spitzmann (1981) (figure 7) and Loponen et al (1982) on Suprasil W, where the results tend to that predicted by (3.10) at time scales below 100 μs at temperatures below 1 K. For longer time scales $C(t)$ changes more rapidly than expected, indicating another contribution to the heat capacity with a relatively well defined minimum relaxation time of about 100 μs at 0.3 K, and which when added to that derived from P gives approximate agreement with long time scale experiments below 1 K.

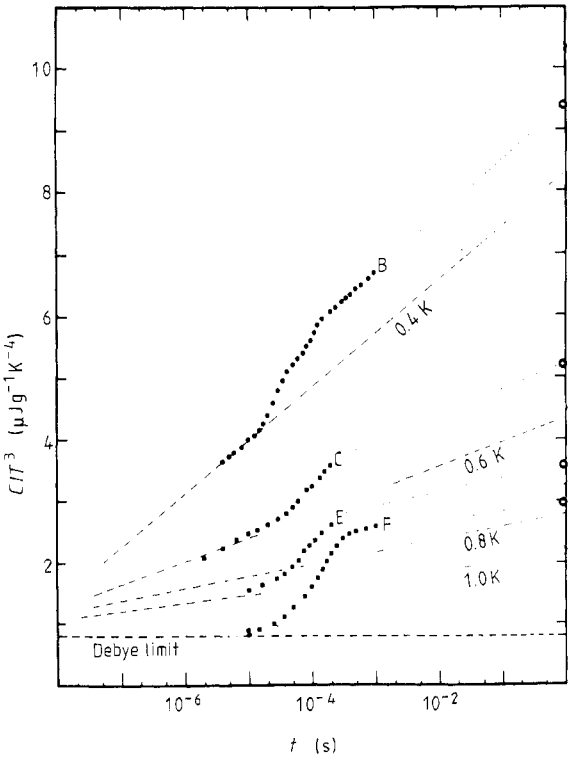

Figure 7. The measured heat capacity of vitreous silica as a function of the time scale of measurement at different temperatures: B 0.4 K; C, 0.6 K; E, 0.89 K; F, 1.0 K. The open circles represent the long-time data, and the broken lines the total heat capacity predicted by the tunnelling model. (Adapted from Meissner and Spitzmann (1981).)

It is worth mentioning at this point that although an all embracing theory based on a single type of tunnelling state is attractive, there is ample evidence to suggest that many different types of impurity could act in this way. It is clear from figure 6, for example, that the presence of water can increase the heat capacity of vitreous silica.

3.3. Thermal expansion

The Gruneisen parameter Γ conveniently relates the measured thermal expansion to microscopic theory. Macroscopically

$$\Gamma = \beta V / \chi_T C_V \tag{3.11}$$

where β is the volume expansivity, χ_T is the isothermal compressibility and C_V is the heat capacity at constant volume of volume V of the solid. Microscopically the significance of Γ can be understood by writing the total entropy of the solid in the quasiharmonic form as $\Sigma_i S_i(\omega_i(V)/T)$ where the normal mode frequencies ω_i are explicit functions only of volume, and where it is understood that experimentally measured frequencies should be used in the formula (Barron 1965, Hui and Allen 1975, Phillips 1981b). Then

$$\left(\frac{\partial S_i}{\partial V}\right)_T = \frac{1}{T} S_i' \left(\frac{\partial \omega_i}{\partial V}\right)_T \tag{3.12}$$

and

$$\left(\frac{\partial S_i}{\partial T}\right)_T = -\frac{\omega_i S_i'}{T^2}$$

where $S_i' = \mathrm{d}S_i(x)/\mathrm{d}x$. Eliminating S_i' and using $C_i = T(\partial S_i/\partial T)_V$ gives

$$\left(\frac{\partial S_i}{\partial V}\right)_V = \frac{-C_i}{\omega_i}\left(\frac{\partial \omega_i}{\partial V}\right)_T$$

which can be summed over i to give

$$\left(\frac{\partial S}{\partial V}\right)_T = -\sum \frac{C_i}{\omega_i}\left(\frac{\partial \omega_i}{\partial V}\right)_T. \tag{3.13}$$

Now

$$\left(\frac{\partial S}{\partial V}\right)_T = -\left(\frac{\partial P}{\partial V}\right)_T \left(\frac{\partial V}{\partial T}\right)_p = -\frac{\beta}{\chi_T}$$

so that with $C_V = \Sigma C_i$, (3.13) becomes

$$\Gamma = \frac{\beta V}{\chi_T C_V} = \frac{-1}{C_V} \sum C_i \partial \ln \omega_i / \partial \ln V. \tag{3.14}$$

Each excitation therefore contributes to the thermal expansion by an amount proportional to the microscopic Gruneisen parameter $-\partial \ln \omega_i / \partial \ln V$, weighted by the contribution of that excitation to the heat capacity.

In crystalline solids (3.14) predicts that β can be calculated from the pressure dependence of the elastic moduli, which determine phonon frequencies at low temperatures. This prediction is confirmed by experiment, but it is not surprising that in glasses, where the heat capacity is dominated by TS below 1 K, anomalous results are found.

Measurements have been made only on a limited number of materials, often with conflicting results, but results for vitreous silica, showing (figure 8) that below 1 K Γ becomes very large and negative, have been confirmed both by measurements of β using a sensitive dilatometer to detect changes of 1 in 10^{12} (Ackerman *et al* 1981) and by direct measurements of Γ using the thermoelastic effect (Wright and Phillips 1984). More generally there seems to be no 'universal' behaviour (Anderson 1986) suggesting that thermal expansion is much more sensitive to details of the microscopic model, including the distribution functions, than are heat capacity and thermal conductivity.

For a tunnelling state with energy $E = \hbar\omega$ the microscopic Gruneisen parameter can be written

$$\Gamma = -\frac{1}{E}\left[\frac{\Delta}{E}\left(\frac{\partial\Delta}{\partial V}\right)_{\Delta_0} + \frac{\Delta_0}{E}\left(\frac{\partial\Delta_0}{\partial V}\right)_{\Delta}\right]. \tag{3.15}$$

Changes in both Δ and Δ_0 with volume can contribute significantly to Γ. The term in Δ, which dominates the interaction Hamiltonian (§ 2.2) leads to Γ for a single tunnelling state of order $10^4/T$, the ratio of $(\partial\Delta/\partial V)$, typically 1 eV, to the energy $E = k_B T$, equal to 10^{-4} at 1 K. However, there is no reason to presuppose a consistent trend among all states for the asymmetry to decrease as the volume is increased, thereby giving a large negative Γ. Formally, the asymmetry contribution to thermal expansion is proportional to $\langle \Delta\gamma_h/E\rangle$, where γ_h is the coupling constant for hydrostatic strain (2.15), in contrast to phonon scattering which is proportional to $\langle \Delta^2\gamma^2/E^2\rangle$. Only if the distribution function for Δ is asymmetric will this term give a non-zero contribution to Γ. However, since the magnitude of Γ is less than 100, this asymmetry need be only 1%, too small for independent measurement by other techniques.

It is known from studies of tunnelling defects in crystals that Δ_0 can be very sensitive to volume changes. In part this results from the exponential dependence on the local potential, but also because this local potential is itself very sensitive to volume. In a crystal, for example, the existence of local multi-minima potentials depends on a

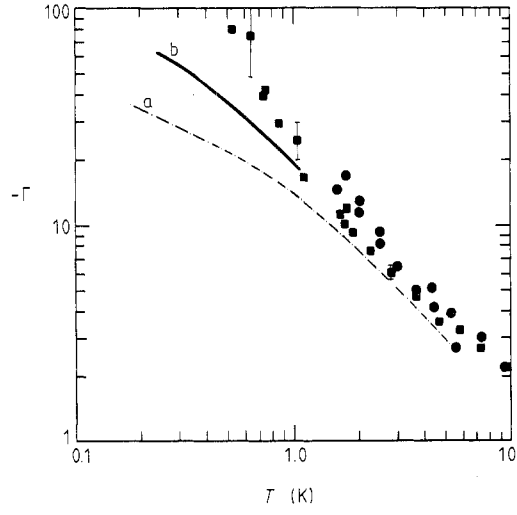

Figure 8. The low-temperature Gruneisen parameter of vitreous silica. The points are from direct measurements in Spectrosil B (squares) and Vitreosil (circles) (Wright and Phillips 1984) and the lines a and b for Spectrosil B and WF respectively are derived from thermal expansion (Ackerman *et al* 1984).

mismatch between the size of the impurity and the space it occupies, so that a very small decrease in volume of the crystal can force the impurity into a central single minimum. Similar arguments may well apply in amorphous solids, so that for a single tunnelling state the factor $(\partial\Delta_0/\partial V)$ can be large. As before, the total contribution will depend on the distribution functions, and is smaller for TS in glasses because for a given E most of the TS have very small values of Δ_0 (Phillips 1973). However, in spite of this reduction the effect of volume changes on Δ_0 appears sufficiently large to explain the observed magnitude of Γ (Wright and Phillips 1984) and also shows, through the variability of local microscopic potentials, why no universal behaviour is expected. This tunnel splitting contribution to Γ should show little temperature dependence, but of course the measured magnitude of Γ increases with decreasing temperature as a result of the increasing contribution of TS to the total heat capacity below 1 K. Experimentally it is observed (figure 8) that Γ is proportional to $T^{-0.5}$ in vitreous silica, suggesting that both asymmetry and tunnel splitting are important. The subtle balance between the various factors explains why Γ varies so much from material to material.

3.4. Energy relaxation and irreversibility

The long relaxation time part of the distribution function (3.8) has been probed in experiments which monitor the flow of energy from a system perturbed from equilibrium (Zimmermann and Weber 1981). If a solid at temperature T_1 is suddenly connected to a reservoir at a slightly lower temperature T_0 ($T_1 > T_0$) by a thermal link of conductance α, the temperature of the sample is normally assumed to relax exponentially with time from T_1 to T_0, ignoring the small change of thermal properties with temperature. In a glass the broad distribution of relaxation times leads to very different behaviour, as shown in figure 9 where for long times the temperature varies as $1/t$, much more slowly than expected.

These results can be understood in terms of the distribution of relaxation times (3.8). The rate at which heat is evolved from the sample is given by $\alpha\dot{T}$, and at long times will be the result of a slow evolution of heat from TS with long relaxation times. Energy associated with the phonons decays exponentially with the thermal time constant, and is negligible at long times. The instantaneous rate of energy loss $\dot{q}$ from

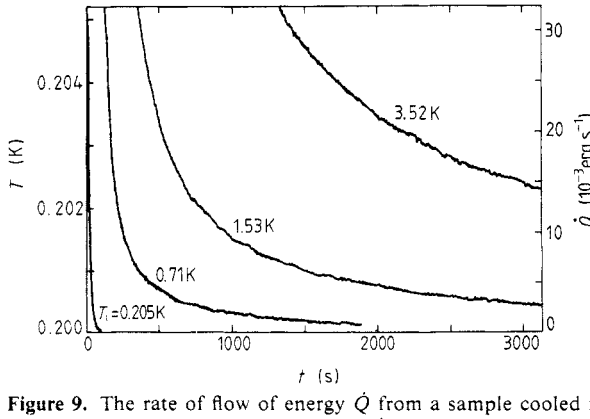

Figure 9. The rate of flow of energy $\dot{Q}$ from a sample cooled from a 'high' temperature, given against each curve, to 0.0200 K. $\dot{Q}$ is measured by monitoring the rate of decrease in temperature, which is non-exponential (Zimmermann and Weber 1981).

a single state of energy E is

$$\dot{q} = E\frac{(p_2 - p_2^0)}{\tau} \tag{3.16}$$

where p_2, the instantaneous value of the occupation probability of the upper state, has time dependence

$$p_2 - p_2^0 = (p_2^1 - p_2^0)\,\mathrm{e}^{-t/\tau} \tag{3.17}$$

and p_2^1 and p_2^0 correspond to equilibrium values at temperatures T_1 and T_0. Summing over all states the total rate of energy loss $\dot{Q}$ per unit volume is given by

$$\dot{Q} = \frac{P}{2}\int_0^\infty \int_{t_{\min}}^\infty E\frac{(p_2^1 - p_2^0)}{\tau}\,\mathrm{e}^{-t/\tau} g(E,\tau)\,\mathrm{d}\tau\,\mathrm{d}E. \tag{3.18}$$

Integrating over τ in the limit $t \gg \tau_{\min}$ (which is always true in these experiments) and using the explicit form of $g(E,\tau)$ from (3.8) gives

$$\dot{Q} = \frac{P}{2t}\int_0^\infty E\left|\frac{1}{1+\exp(E/k_B T_1)} - \frac{1}{1+\exp(E/k_B T_0)}\right|\mathrm{d}E. \tag{3.19}$$

Finally

$$\dot{Q}(T_1, t) = \frac{\pi^2}{24} P k_B^2 (T_1^2 - T_0^2) t^{-1}. \tag{3.20}$$

Equation (3.20) agrees well with the results both in magnitude and time dependence, and the derivation shows how a broad distribution of relaxation times leads quite generally to a t^{-1} dependence. These experiments demonstrate clearly the existence of long relaxation times in glasses, up to 5×10^3 s at 1 K.

Associated with $\dot{Q}$ is an increase in entropy, and one interesting aspect of a two-level system is that entropy changes and irreversibility can be followed in detail (Wright and Phillips 1984). This is possible because the thermodynamic properties are uniquely specified by the instantaneous occupation probability p which plays the role of an internal variable in general irreversible thermodynamics. For a subset of TS with energy E and relaxation time τ an effective temperature T' can be defined by

$$\frac{E}{k_B T'} = \ln[(1-p)/p] \tag{3.21}$$

$$= \ln[(1-p_0)/p_0] + \frac{1}{k_B T_0}\left(\frac{\partial E}{\partial p_0}\right)\delta p \tag{3.22}$$

where $\delta p = p - p_0$ is a small departure from the equilibrium value p_0. The energy flow $\dot{q} = E\dot{p}$ results in a rate of entropy change

$$\dot{S} = -E\dot{p}\left(\frac{1}{T'} - \frac{1}{T_0}\right) \tag{3.23}$$

$$= \frac{1}{T_0}\left(\frac{\partial E}{\partial p_0}\right)\frac{(\delta p)^2}{\tau}. \tag{3.24}$$

In an experiment such as that described at the beginning of this section, the entropy changes can be followed from a knowledge of the variation of $p - p_0$. For larger departures from equilibrium (3.21) and (3.23) can be used without assuming δp is small. This analysis has been used to relate thermoelastic processes measured under different experimental conditions (Wright 1986, Wright and Phillips 1984).

4. Response to external fields

The response of two-level systems to external fields is a problem that has been treated extensively in connection with the interaction of light with atoms and in magnetic resonance. Although the basic ideas are the same for TS in glasses, additional features arise because of the strong coupling to phonons, and because of the broad distribution of energies and relaxation times. The interaction with both acoustic and electric fields has been intensively studied, although the electrical case has the important simplification from both experimental and theoretical points of view that the fields are uniform across the sample. In most of § 4 we will present the argument for the electrical case, extending where necessary to acoustic fields.

4.1. Weak fields

In this limit the interaction can be considered as in § 2.2 by ignoring the phase relationship between the wavefunctions describing the two energy levels. This is possible when the perturbation produced by the external field is small, a condition that is defined more precisely in § 4.2. In this limit the attenuation is given in the acoustic case by (3.4)

$$l^{-1} = \left(\frac{\pi\gamma_\alpha^2\omega}{\rho v_\alpha^3}\right) P \tanh(\hbar\omega/2k_B T). \tag{3.4}$$

The equivalent result for electric fields is obtained on replacing γ_α by the dipole moment p_0 (see (2.15)) and the amplitude of the strain field $(\hbar\omega/2\rho v_\alpha^2)^{1/2}$ by the equivalent electric field amplitude $(\hbar\omega/2\varepsilon_0\varepsilon_r)^{1/2}$, where ε_r is the relative dielectric constant. The attenuation coefficient α is given by

$$\alpha = \left(\frac{\pi p_0^2\omega}{3c\varepsilon_0\varepsilon_r}\right) P \tanh(\hbar\omega/2k_B T) \tag{4.1}$$

where c is the velocity of light in the solid and the factor of three arises from averaging $(\boldsymbol{p}_0 \cdot \boldsymbol{\xi})$ over relative orientations. Both (3.4) and (4.1) have been tested experimentally (Golding *et al* 1976b, Schickfus and Hunklinger 1977) taking care at low temperatures to satisfy the weak field condition. Results for l_α^{-1} in the acoustic case (figure 10) show not only the predicted tanh dependence on $\hbar\omega/k_B T$ but also give values of $P\gamma^2$ which

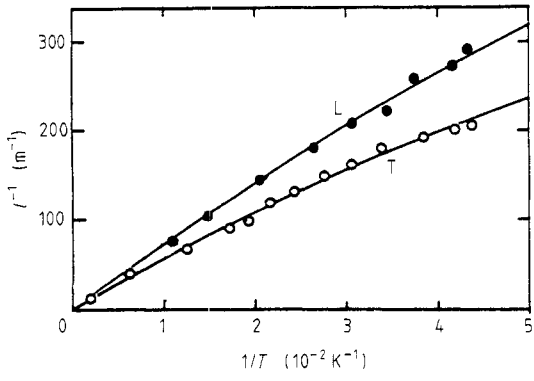

Figure 10. The phonon free path l^{-1} for transverse and longitudinal waves at 0.6 GHz plotted against $1/T$ (Golding *et al* 1976b).

can be used to calculate a value for the thermal conductivity within a factor of two of the measured value. The slight energy dependence of P, implicit in the departure from a T^2 dependence of $\kappa(T)$, is such as to improve the agreement between parameters measured in acoustic measurements at 0.6 GHz and those contributing to $\kappa(T)$ at 1 K.

Associated with the absorption is a temperature-dependent variation of velocity. The velocity, calculated from the real part of the response function, is given by the Kramers-Kronig relation (Landau and Lifshitz 1984) as

$$\Delta v(\omega) = \frac{1}{\pi} \int_0^\infty \frac{v^2 l^{-1}(\omega')}{\omega^2 - \omega'^2} \, d\omega' \tag{4.2}$$

where the principal part of the integral is to be taken. Using (3.4) for l^{-1} and measuring $v(T)$ with respect to $T = 0$, the velocity is given by (Hunklinger and Arnold 1976)

$$v(T) - v(0) = \frac{P\gamma^2}{\rho v}\left[\text{Re}\,\Psi\left(\frac{1}{2} + \frac{\hbar\omega}{2\pi i k_B T}\right) - \ln\frac{\hbar\omega}{k_B T}\right] \tag{4.3}$$

where Ψ is the digamma function (Abramowitz and Stegun 1964). The first term is important only for $\hbar\omega$ comparable to $k_B T$, which for frequencies of 1 GHz means working at temperatures below 50 mK. Such measurements (figure 11) confirm the detailed form of (4.3) (Golding *et al* 1976a) but in most experiments it is sufficient to use the result for $\hbar\omega \ll k_B T$, referring the velocity to a temperature T_0 to give

$$v(T) - v(T_0) = \frac{P\gamma^2}{\rho v} \ln(T/T_0). \tag{4.4}$$

This equation has been used extensively to derive values of $P\gamma^2$ even in materials such as amorphous metals (§ 6) where the contribution of TS to the thermal properties is

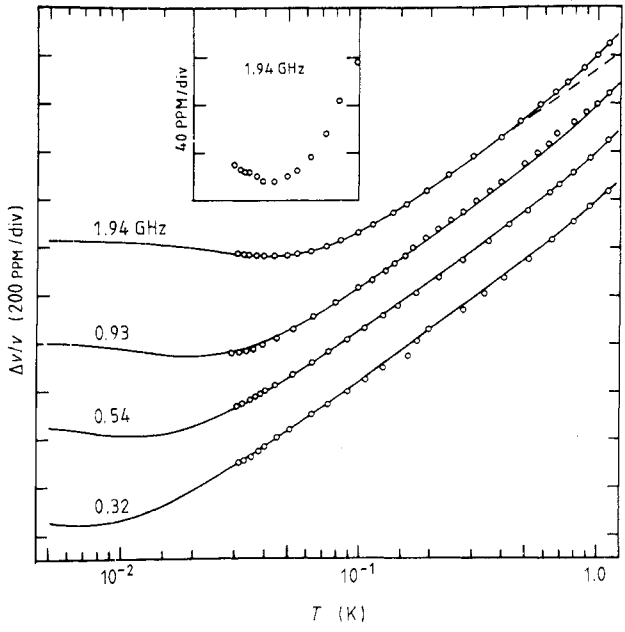

Figure 11. The variation of acoustic velocity with temperature between 25 mK and 1 K (Golding *et al* 1976a).

difficult to identify. One feature that makes (4.4) particularly useful is that it is insensitive to the strength of the acoustic intensity. The reason for this is that the major contribution to the integral (4.2) comes from states for which $\hbar\omega/k_B T$ is close to unity, and which are therefore much more difficult to saturate than those for which $\hbar\omega \ll k_B T$. This feature also means that the TS sampled in a typical velocity measurement at frequency ω have a larger energy splitting than those probed in attenuation measurements at the same frequency. Derived values of $P\gamma^2$ therefore need not be identical in the two experiments if P is energy dependent.

The electrical equivalent of (4.4) can be expressed in terms of the relative dielectric constant $\varepsilon_r(T)$ as

$$\varepsilon_r(T) - \varepsilon_r(T_0) = \frac{2}{\varepsilon_0} p_0^2 P \ln(T/T_0). \tag{4.5}$$

Experimental results shown in figure 12 confirm the form (4.5) and also demonstrate the additional information obtainable by measuring both acoustic and electrical properties. Different types of silica give almost the same curve for the variation of acoustic velocity, but figure 12 shows clearly that the contribution of TS to the dielectric constant is proportional to the concentration of water, probably as OH groups. This has been interpreted as additional TS produced by hindered OH rotation (Phillips 1981c).

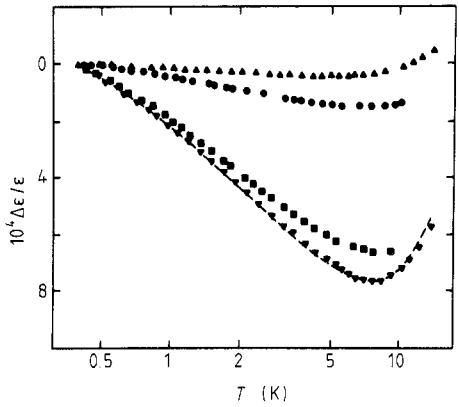

Figure 12. The temperature variation of the dielectric constant of vitreous silica containing differing concentrations of hydroxyl (▲, <1.5 PPM: ●, 190 PPM; ■, 1000 PPM; ▼, 1200 PPM) (Schickfus and Hunklinger 1976).

4.2. Strong fields

The response to large applied fields is critically dependent on the coherence between the two eigenfunctions ψ_1 and ψ_2 (§ 2.2) and can be treated only by solving the coupled equations for the time evolution of the probability amplitudes a_1 and a_2. Formal methods for solving the problem developed for optical saturation (Sargent *et al* 1974) and magnetic resonance (Slichter 1980) have been applied to TS in glasses (Golding and Graebner 1981) but for completeness we will present here a relatively straightforward approach for a spatially homogeneous electric field. The response to the perturbation $H_{int}(t)$ is determined by the parameters $p_1 = -p_2 = \langle\psi_1|qx|\psi_1\rangle$ and $p_{12} = p_{21} = \langle\psi_1|qx|\psi_2\rangle$, where q is the charge associated with the tunnelling particle.

Using the general state function (2.12) in the time-dependent Schrödinger equation

$$(H_0 + H_{\text{int}}(t))\Psi = \mathrm{i}\hbar \frac{\partial \Psi}{\partial t} \tag{4.6}$$

gives equations for $\dot{a}_1$ and $\dot{a}_2$:

$$\dot{a}_1 = \frac{1}{\mathrm{i}\hbar}[\langle \psi_1 | H_{\text{int}}(t) | \psi_1 \rangle a_1 + \langle \psi_1 | H_{\text{int}}(t) | \psi_2 \rangle a_2 \exp(-\mathrm{i}\omega_0 t)] \tag{4.7}$$

$$\dot{a}_2 = \frac{1}{\mathrm{i}\hbar}[\langle \psi_1 | H_{\text{int}}(t) | \psi_2 \rangle a_1 \exp(\mathrm{i}\omega_0 t) + \langle \psi_2 | H_{\text{int}}(t) | \psi_2 \rangle a_2]. \tag{4.8}$$

Writing $H_{\text{int}}(t) = -\xi(t) qx$ and considering for simplicity the symmetric double well where $p_1 = p_2 = 0$ (for a more general discussion see Pippard 1983), the equations become

$$\dot{a}_1 = \frac{-\xi(t) p_{12}}{\mathrm{i}\hbar} a_2 \exp(-\mathrm{i}\omega_0 t) \tag{4.9}$$

$$\dot{a}_2 = \frac{-\xi(t) p_{12}}{\mathrm{i}\hbar} a_1 \exp(\mathrm{i}\omega_0 t). \tag{4.10}$$

The time-dependent dipole moment from (2.13) is given by u, where

$$u = a_1 a_2^* \exp(\mathrm{i}\omega_0 t) + a_2 a_1^* \exp(-\mathrm{i}\omega_0 t). \tag{4.11}$$

Using (4.9) and (4.10),

$$\dot{u} = \mathrm{i}\omega_0 [a_1 a_2^* \exp(\mathrm{i}\omega_0 t) - a_2 a_1^* \exp(-\mathrm{i}\omega_0 t)] = \omega_0 v \tag{4.12}$$

where $v = \mathrm{i}[a_1 a_2^* \exp(\mathrm{i}\omega_0 t) - a_2 a_1^* \exp(-\mathrm{i}\omega_0 t)]$. In a similar way

$$\dot{v} = \frac{2\xi(t) p_{12}}{\hbar} w - \omega_0 u \tag{4.13}$$

where $w = a_1 a_1^* - a_2 a_2^*$, and

$$\dot{w} = -\frac{2\xi(t)}{\hbar} p_{12} v. \tag{4.14}$$

Only the interaction with the driving field has been included in (4.12)-(4.14), but the incoherent interaction with thermal phonons can be included by introducing phenomenological relaxation times T_1 and T_2. The population difference w relaxes back to the equilibrium value $w_0 = -\tanh(E/2k_B T)$, where $E = \hbar\omega_0$, with a relaxation time T_1 given by (2.26). The off-diagonal coherence between ψ_1 and ψ_2 relaxes back to zero with a time constant T_2, known as the dephasing time. The resulting equations are then

$$\dot{u} = -\frac{u}{T_2} + \omega_0 v \tag{4.15}$$

$$\dot{v} = -\frac{v}{T_2} - \omega_0 u + \frac{2\xi(t) p_{12}}{\hbar} w \tag{4.16}$$

$$\dot{w} = -\frac{(w - w_0)}{T_1} - \frac{2 p_{12} \xi(t)}{\hbar} v. \tag{4.17}$$

Equations (4.15)-(4.17) are the Bloch equations of magnetic resonance.

In the steady state, when transient effects governed by T_1 and T_2 have decayed to zero, we can look for steady state solutions. In the absence of a driving field only w is non-zero, so that both u and v will vary at least linearly with $\xi(t)$. The final term in (4.17) is therefore quadratic in ξ, and will give a steady average value $\bar{w}$ which differs from w_0. With $w = \bar{w}$ and constant in (4.16),

$$\dot{\rho} = \dot{u} + i\dot{v} = -\frac{\rho}{T_2} - i\omega_0\rho + \frac{2i\xi(t)p_{12}}{\hbar}\bar{w}. \tag{4.18}$$

For a driving field $\xi(t) = \xi_0[\exp(i\omega t) + \exp(-i\omega t)]$ the second exponential term governs the behaviour of $\rho = \rho_0 \exp(-i\omega t)$, giving

$$\rho_0 = \frac{(2i\xi_0 p_{12} T_2 \bar{w})}{\hbar} \frac{1}{[1 + i(\omega_0 - \omega)T_2]}. \tag{4.19}$$

The imaginary part of ρ_0 gives the amplitude of v which when introduced into (4.17) gives a value for $\bar{w}$ of

$$\bar{w} = w_0\left(1 + \frac{4p_{12}^2 \xi_0 T_1 T_2}{\hbar^2} \frac{1}{[1 + (\omega_0 - \omega)^2 T_2^2]}\right)^{-1}. \tag{4.20}$$

The result for ρ_0 shows, after substitution of (4.20) in (4.19), that the response at resonance is reduced at large fields by a factor $[1 + (2p_{12}\xi_0/\hbar)^2 T_1 T_2]$ and that the response curve is broadened, defining an effective relaxation time T_2' where

$$\frac{1}{T_2'^2} = \frac{1}{T_2^2} + \frac{(2p_{12}\xi_0)^2}{\hbar^2} \frac{T_1}{T_2}. \tag{4.21}$$

In a glass the total response is the sum of contributions from states which are within a linewidth of the exciting frequency ω. The number of these states, of order $P(\hbar/T_2')$ where P is the constant density of states, is increased at large fields by a factor T_2'/T_2. However, because the contribution of each is reduced by a factor $(T_2/T_2')^2$, the effect of a large field is to reduce the attenuation by a factor

$$\frac{T_2}{T_2'} = \left(1 + \frac{(2p_{12}\xi)^2}{\hbar^2} T_1 T_2\right)^{1/2}. \tag{4.22}$$

Equation (3.4) must therefore be modified to give

$$l_\alpha^{-1} = \frac{(\pi\gamma_\alpha^2 \omega)}{(\rho v_\alpha^3)} \frac{P \tanh(\hbar\omega/2k_B T)}{(1 + I/I_c)^{1/2}} \tag{4.23}$$

where in the acoustic case the intensity ratio

$$I/I_c = \frac{(2\gamma e)^2}{\hbar^2} T_1 T_2 \tag{4.24}$$

with $I = 2\rho e_0^2 v^3$ (in W m^{-2}) for a strain field $2e_0 \cos \omega t$ and where

$$I_c = \hbar^2 \rho v^3 / 2\gamma^2 T_1 T_2. \tag{4.25}$$

In the electrical case

$$I_c = 3\hbar^2 \varepsilon_r \varepsilon_0 c / 2p_0^2 T_1 T_2 \tag{4.26}$$

after averaging over dipole orientations, and where p_{12} has been replaced by p_0 used earlier.

Equation (4.24) can be given a simple physical interpretation. The cross-over between weak and strong fields occurs when the acoustic-phonon energy per unit frequency range is equal to that of thermal phonons. If the critical energy density is E_c then for $\hbar\omega \ll k_B T$

$$(E_c/\hbar\omega T_2^{-1}) = (\omega^2/\pi v_\alpha^3)(k_B T/\hbar\omega)$$

if the energy width of the acoustic pulse is determined by T_2 and not by the pulse length. The critical intensity is

$$I_c = v_\alpha E_c = (\omega^2 k_B T/\pi v_\alpha T_2)$$

which on using (2.26) with $E = \Delta_0 = \hbar\omega$, gives a result of the same form as (4.25).

Saturation has been observed in both electrical (Schickfus and Hunklinger 1977) and acoustic experiments (Hunklinger *et al* 1972, Golding *et al* 1973, 1976b, Graebner *et al* 1983) below 1 K (figure 13). In general the agreement with (4.23) is good, although at very low temperatures the steady state solutions of the Bloch equations, assumed in deriving (4.23), may not apply if the length of the acoustic pulse is less than T_1.

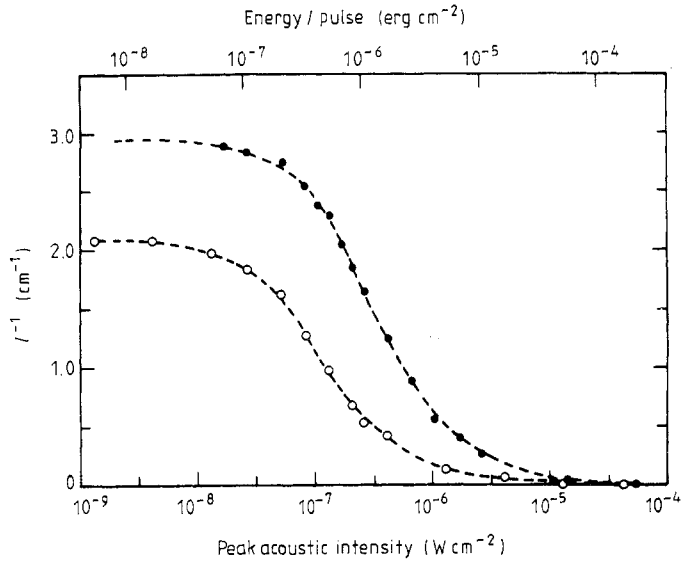

Figure 13. Acoustic attenuation as a function of acoustic intensity in vitreous silica (Golding *et al* 1976b). $T = 0.023$ K. ●, transverse, $\omega/2\pi = 0.534$ GHz; ○, longitudinal $\omega/2\pi = 0.592$ GHz.

4.3. Relaxation

Two-level systems can give a large response in non-resonant electric and acoustic fields. Formally this can be treated together with resonant processes by solving the Bloch equations (Jackle *et al* 1976) but in practice it is convenient to treat the two separately. The distinction can most easily be seen by subjecting a thermal distribution of tunnelling states of energy E, asymmetry Δ to a step function field. In the electrical case the dipole moment in the absence of the field vanishes for a random angular distribution

of the dipole moments, where each dipole is $p_0\Delta/E$ (2.9). Considering only those pointing along the field, in thermal equilibrium the average moment is

$$\bar{p} = p_0 \frac{\Delta}{E} \tanh\left(\frac{E}{2k_B T}\right) \tag{4.27}$$

and the mean polarisability is given by

$$\bar{\alpha} = \frac{d\bar{p}}{d\xi} = 2p_0 \frac{d\bar{p}}{d\Delta}$$

where the effect of the field is to change the asymmetry by $2p_0\xi$. Using (4.27) gives for the average contribution from all states

$$\bar{\alpha} = \frac{2p_0^2}{3} \frac{\Delta_0^2}{E^3} \tanh\left(\frac{E}{2k_B T}\right) + \frac{p_0^2}{3k_B T} \frac{\Delta^2}{E^2} \operatorname{sech}^2\left(\frac{E}{2k_B T}\right) \tag{4.28}$$

where the factor of three comes from averaging over orientation. The first term in (4.28) reflects the change in the dipole moment of each state, and the second the effect of redistribution between the energy levels when the system moves out of thermal equilibrium as E is changed. The redistribution occurs relatively slowly on a time scale determined by coupling to the surroundings, while the change in dipole moment occurs on a time scale $\hbar/E$. In fact (4.28) represents a time average on a scale longer than $\hbar/E$, and the time response is oscillatory, as shown in figure 14. For non-resonant fields the dominant response is by relaxation, represented by the second term of (4.28).

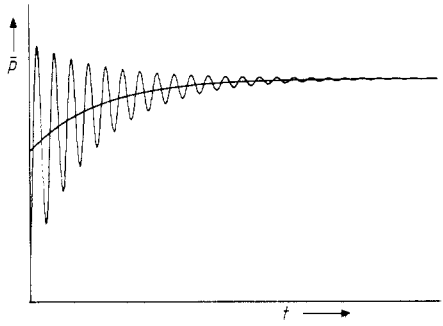

Figure 14. The response of a two-level system to a step-function applied electric field, showing the rapid oscillatory resonant variation of the average dipole moment together with the slower variation arising from relaxation (after Pippard 1983).

With this preamble, it is possible to write down an equation governing the population difference w between the two levels. Relaxation proceeds according to

$$\dot{w} = -\frac{w - \bar{w}(t)}{\tau} \tag{4.29}$$

where $\bar{w}$ is the instantaneous equilibrium value of the population difference, given in the electrical case by

$$\bar{w} = w_0 + \frac{\partial w_0}{\partial \Delta} 2p_0\xi(t) \tag{4.30}$$

and τ is conventionally written for the relaxation time T_1. Combining (4.29) and (4.30) gives for $\delta w = w - w_0$,

$$\tau \delta \dot{w} = -\delta w + \frac{\partial w_0}{\partial \Delta} 2p_0 \xi(t). \tag{4.31}$$

For $\xi(t) = \xi_0 \exp(-i\omega t)$ the solution is of the form

$$\delta w = \frac{\partial w_0}{\partial \Delta} 2p_0 \frac{\xi_o \exp(-i\omega t)}{1 - i\omega t}.$$

The corresponding change in average dipole moment $\delta p(\omega) = p_0(\Delta/E)\, \delta w$ defines a complex susceptibility $\chi(\omega) = \delta p(\omega)/\xi(\omega)$, where

$$\chi(\omega) = \frac{\chi(0)}{1 - i\omega t} \tag{4.32}$$

with

$$\chi(0) = \frac{p_0^2}{3k_B T} \frac{\Delta^2}{E^2} \operatorname{sech}^2\left(\frac{E}{2k_B T}\right). \tag{4.33}$$

In the acoustic case an equivalent calculation gives the same form for $\chi(\omega)$ (equivalent to the modulus) with $p_0^2/3$ replaced by γ^2 (where the orientational average is incorporated). Restricting attention to the acoustic case, where most experimental information is available, and using the results

$$\alpha = \frac{\omega \chi''(\omega)}{\rho v^3}$$

and

$$\frac{\Delta v}{v} = \frac{\chi'(\omega)}{2\rho v^2}$$

where $\chi'(\omega)$ and $\chi''(\omega)$ are the real and imaginary parts of $\chi(\omega)$, gives, after introducing the distribution function $g(E, \tau)$,

$$\alpha = \frac{\gamma^2}{\rho v^3 k_B T} \int_0^\infty \int_{\tau_{min}}^\infty (1 - \tau_{min}/\tau) \operatorname{sech}^2\left(\frac{E}{2k_B T}\right) \frac{\omega^2 \tau}{1 + \omega^2 \tau^2} g(E, \tau)\, d\tau\, dE \tag{4.34}$$

where Δ^2/E^2 is replaced by $(1 - \tau_{min}/\tau)$. Equation (4.34) can be evaluated analytically in the limits $\omega\tau_{min} \ll 1$ and $\omega\tau_{min} \gg 1$ to give

$$\alpha = \frac{(\gamma^2 P)}{(\rho v^2)} \frac{\pi \omega}{2v} \qquad \omega\tau_{min} \ll 1 \tag{4.35}$$

and

$$\alpha = \frac{\pi^3}{24} \frac{\gamma^2 P}{\rho^2 v^3 \hbar^4} \left(\sum_\alpha \frac{\gamma_\alpha^2}{v_\alpha^5}\right) k_B^3 T^3 \qquad \omega\tau_{min} \gg 1 \tag{4.36}$$

using (2.26) for τ_{min} with $\Delta_0 = E$. No saturation is usually expected for these relaxation contributions to the attenuation because the driving field does not itself cause transitions between the two energy levels.

The corresponding velocity changes can be calculated in the same limits. For $\omega\tau_{\min} \gg 1$ the effect of relaxation processes on the velocity is small in comparison to the resonant process, but for $\omega\tau_{\min} \ll 1$

$$\frac{\Delta v}{v} = \frac{(P\gamma^2)}{(2\rho v^2)} \frac{1}{2k_B T} \int_0^\infty \int_{\tau_{\min}}^\infty \operatorname{sech}^2\left(\frac{E}{2k_B T}\right)\left(1 - \frac{\tau_{\min}}{\tau}\right)\frac{1}{1+\omega^2\tau^2} g(E,\tau)\, d\tau\, dE$$

$$= -\frac{(P\gamma^2)}{(\rho v^2)} \frac{3}{2} \ln(T/T_0) \tag{4.37}$$

for $\omega\tau_{\min} \ll 1$ and $\hbar\omega < k_B T$, where T_0 is a reference temperature. This result has the same form as that for resonant scattering, and differs only by a factor of $\frac{3}{2}$. The factor 3 is a direct consequence of the T^3 dependence of $\tau_{\min}$, so that higher-order phonon processes will give an even more rapid negative change of velocity with temperature.

At any temperature $\tau_{\min}$ can be estimated from (2.26) with $E = \Delta_0 = k_B T$ as approximately 1 ns at 1 K, varying as T^{-3}, so that $\omega\tau_{\min}$ for a typical ultrasonic frequency of 100 MHz is unity just above this temperature. The regime $\omega\tau_{\min} \gg 1$ therefore coincides with the onset of higher-order phonon processes, which cannot generally be included by a simple power law dependence of $\tau_{\min}$ on temperature. However, a maximum in $\Delta v/v$ occurs when the effect of relaxation dominates the logarithmic resonant contribution to $\Delta v/v$ seen at lower temperatures. The temperature of this maximum gives another way of estimating coupling constants, using (2.26) and the condition $\omega\tau_{\min} \sim 1$ (Hunklinger and Raychaudhuri 1986).

In order to examine in detail the accuracy of (4.34)-(4.36) measurements must be made at low frequencies. This has been done at about 1 kHz (Raychaudhuri and Hunklinger 1984) and close to 1 Hz (Wright and Phillips 1984), where $\omega\tau_{\min}$ is unity at 20 mK and 2 mK respectively. Results at 1 kHz shown in figure 15 demonstrate the two expected logarithmic regimes. The combination of opposing resonant and relaxation terms (4.4) and (4.37) observed above 100 mK gives as expected a slope half that of the resonant term alone below 100 mK. At these low frequencies the attenuation is more conveniently described by the quality factor Q where

$$Q^{-1} = \frac{\alpha v}{\omega} = \frac{\pi}{2} \frac{(P\gamma^2)}{(\rho v^2)}. \tag{4.38}$$

The frequency independence of Q for $\omega\tau_{\min} \gg 1$ is confirmed by experiment and takes a value of about 3.5×10^{-4} below 4 K in silica. Although the average γ^2 entering (4.38)

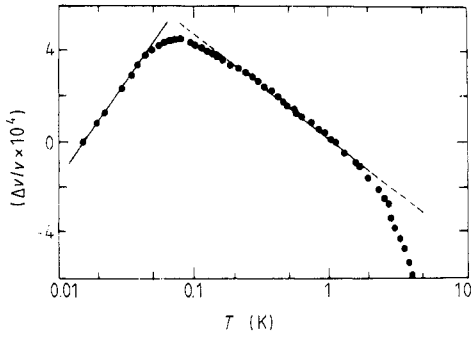

Figure 15. The temperature variation of the velocity of sound measured at low frequencies, showing the two logarithmic regimes with slopes in the ratio −2 (Hunklinger and Raychaudhuri 1986). Cover glass 1028 Hz.

differs for different experimental techniques, the values of $P\gamma^2$ in SiO_2 are in good agreement with those derived from high-frequency velocity measurements. At lower temperatures (Raychaudhuri and Hunklinger 1984) Q^{-1} falls as T^3 in accord with (4.36).

In contrast to these very-low-frequency examples, relaxation attenuation of thermal phonons can be a significant contribution to the total scattering at a few degrees, and can give a decrease with increasing temperature of the thermal conductivity κ. Even though extension of relaxation effects to frequencies above 10^{10} Hz involves an extrapolation of (2.26) and (4.36) into regimes where no independent test of their validity is possible, fitting to thermal conductivity data gives reasonable agreement with predicted values (Zaitlin and Anderson 1975).

5. Pulse echo experiments

5.1. General theory

In contrast to the steady state response to large applied fields discussed in § 4.2, this section concentrates on pulse phenomena where the pulse length τ_p is less than either T_1, T_2 or both. The experiments can be understood in terms of an analysis based on (4.9) and (4.10), which for a resonant applied field $\xi_0[\exp(i\omega_0 t)+\exp(-i\omega_0 t)]$ take the form, with neglect of the non-resonant exponent,

$$\dot{a}_1 = -\frac{\xi_0 p_{12}}{i\hbar} a_2 \tag{5.1}$$

$$\dot{a}_2 = -\frac{\xi_0 p_{12}}{i\hbar} a_1. \tag{5.2}$$

Combining these equations gives

$$\ddot{a}_1 = -(\xi_0 p_{12}/\hbar)^2 a_1 = -\omega_1^2 a_1 \tag{5.3}$$

and similarly for a_2 where $\omega_1 = \xi_0 p_{12}/\hbar$. If the system is initially in state ψ_1, the wavefunction at time t later is

$$\Psi(t) = \cos(\omega_1 t)\psi_1 \exp(i\omega_0 t/2) + \sin(\omega_1 t)\psi_2 \exp(-i\omega_0 t/2). \tag{5.4}$$

After a time $\pi/2\omega_1 = \pi\hbar/2\xi_0 p_{12}$ the system is in the state ψ_2. After a $\pi/2$ pulse, of length $\pi/4\omega_1$, the system is in a mixed state $(\psi_1+\psi_2)/\sqrt{2}$, assuming that relaxation can be neglected during the pulse, i.e. $\tau_p \ll T_1$ and T_2.

A typical experiment consists of a $\pi/2$ pulse followed a time t_0 later by a π pulse. At the end of the first pulse the wavefunction is in the state $(\psi_1+\psi_2)/\sqrt{2}$ if $\omega_1\tau_p \ll 1$, and after a time t_0 has evolved into

$$\Psi(t_0) = (1/\sqrt{2})[\psi_1 \exp(i\omega_0 t_0/2) + \psi_2 \exp(-i\omega_0 t_0/2)].$$

During the second pulse the probability amplitudes must satisfy (5.1) and (5.2), so that

$$\Psi(t) = (1/\sqrt{2})\{\psi_1 \cos[\omega_1(t-t_0)] + \psi_2 \sin[\omega_1(t-t_0)]\} \exp(i\omega_0 t_0/2)$$
$$+ (1/\sqrt{2})\{\psi_1 \sin[\omega_1(t-t_0)] + \psi_2 \cos[\omega_1(t-t_0)]\} \exp(-i\omega_0 t_0/2)$$
$$t_0 < t < t_0 + 2\tau_p$$

and at the end of the pulse

$$\Psi(t_0+2\tau_p) = (1/\sqrt{2})[\psi_2 \exp(i\omega_0 t_0/2) + \psi_1 \exp(-i\omega_0 t_0/2). \tag{5.5}$$

The subsequent time variation has the form for $t_0 \gg \tau_p$

$$\Psi(t) = (1/\sqrt{2})\{\psi_2 \exp(i\omega_0 t/2) \exp[-i\omega_0(t-t_0)/2] + \psi_1 \exp(-i\omega_0 t/2) \exp[i\omega_0(t-t_0)/2]\}. \quad (5.6)$$

The dipole moment $\langle p \rangle$ can be calculated as in § 2.2, and will be a maximum when $a_1 = a_2 = 1/\sqrt{2}$, at time $t = 2t_0$. The signal produced at $t = 2t_0$ is known as a spontaneous echo. For a single subset of TS with energy $E = \hbar\omega_0$ this maximum would not be sharp, but because it occurs at a time independent of ω_0 it is very sharp in an amorphous solid where TS with a range of energies are inevitably excited as a result of the finite length of the pulse. One of the fascinating aspects of echo phenomena is the way in which a broad distribution of parameters leads directly to the sharpness of the response.

This analysis has ignored the effect of relaxation, justifiable during short pulses if $\tau_p \ll T_1$ and T_2, but which must be included during the time interval $2t_0$. Both the energy exchange with phonons, which contributes to T_1 and T_2, and interaction between TS which produces dephasing important in T_2, reduce the echo amplitude. Indeed, as will be described in the next section, by a suitable choice of pulse pattern either T_1 or T_2 can be measured.

5.2. Echo experiments

Photon and phonon echoes can be observed only at very low temperatures. Unlike the equivalent magnetic experiment where the large steady field prepares the system in a well defined initial state, in amorphous solids each TS can be prepared in state ψ_1 only by cooling to a temperature T less than $\hbar\omega/k_B$, where ω is the angular frequency of the exciting pulses. For example, in a typical spontaneous electric echo experiment, similar to that analysed in § 5.1, two pulses of length τ_p and $2\tau_p$ (typically <100 ns) at a frequency of 1 GHz ($\hbar\omega/k_B \sim 40$ mK) are applied across a capacitor containing the sample at a temperature of 10–20 mK in a dilution refrigerator. At these temperatures τ_p is less than T_1 or T_2 so that relaxation can be ignored during the pulse. The echo amplitude is observed as a function of ξ_0, the electric field amplitude, or t_0, the time between pulses.

Echo experiments on TS have been designed to give different kinds of information. The amplitude of the echo as a function of the strength of the applied resonant field gives a measure of the induced electric dipole moment or the phonon coupling constant, the echo amplitude as a function of pulse separation in a two- or three-pulse experiment can be used to give T_2 or T_1 respectively. Analysis of these experiments follows the equivalent magnetic case, except that the TS problem is complicated by three factors. First, the elastic or electric dipoles are not aligned with respect to the driving field and a calculation of the echo amplitude involves an average over orientation. Secondly, for a given resonant frequency ω_0 there exists a distribution of induced moments (elastic or electric) and relaxation times which should be included in the analysis. Finally, in electric echo experiments the local field seen by the TS is not equal to the applied field, and a local-field correction factor must be used when evaluating absolute values of the dipole moment.

The various experimental and theoretical complications and the relative scarcity and inconsistency of results make it inappropriate to analyse and compare in detail the experimental results. In this and the next section the emphasis is on basic physical ideas at the cost of idealising what is still a confusing experimental and theoretical problem.

The echo amplitude measured for small pulse separations in an ideal double-pulse experiment, ignoring relaxation, is a maximum (from the analysis given in § 5.1) when the amplitude of the driving field ($2\xi_0 \cos(\omega\tau)$ or $2e_0 \cos(\omega\tau)$) is given by

$$\omega_1 \tau_p = \frac{\xi_0 p_{12} \tau_p}{\hbar} = \frac{\pi}{4} \tag{5.7}$$

in the electric case, or

$$\frac{e_0 \gamma \tau_p}{\hbar} = \frac{\pi}{4} \tag{5.8}$$

for acoustic pulses. (Experimentally it is often convenient to use two identical pulses, in which case the echo amplitude is a maximum when $\omega_1 \tau_p = 2\pi/3$.) The relationship between p_{12}, derived from (5.7), and p_0, derived from an attenuation or velocity measurement (4.1) or (4.5), is not straightforward because averages over the distribution functions are weighted differently in the two cases. For example, analysis of an electric echo experiment has shown that $p_{12} = 0.6\, p_0$ (Phillips 1981c), although in practice experimental difficulties involved in an accurate determination of ξ_0 or e_0 give the greatest uncertainties in the derived values of p_0 or γ.

Typical results for the electric echo amplitude as a function of ξ_0 are shown in figure 16. It is clear that two distinct dipole species exist in those samples of silica (Suprasil I and Herasil) that contain OH groups, with dipole moments differing by a factor of six. The larger moment of approximately 5×10^{-30} C m (taking into account local field factors) has been associated with rotation of the proton in OH (Phillips 1981c), but the smaller dipole appears to be intrinsic to silica. By adjusting the frequency and magnitude of acoustic or electric fields particular TS can be selected from broad distributions by means of their energy and coupling strength. This selectivity of echo experiments is in marked contrast to most experimental studies of the amorphous state.

The variation of the echo amplitude with separation of two equal pulses is shown in figure 17 for the acoustic case (Graebner and Golding 1979) with the field adjusted

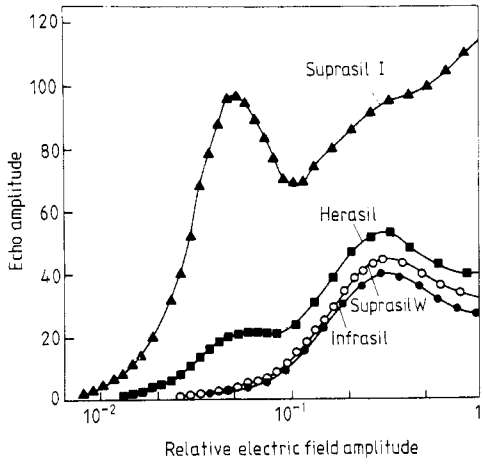

Figure 16. Amplitude of the spontaneous electric echo in different samples of vitreous silica (Golding *et al* 1979). The OH content of the samples is as follows: Suprasil I 1200 PPM, Herasil 200 PPM, Suprasil W and Infrasil less than 10 PPM. $T = 19$ mK.

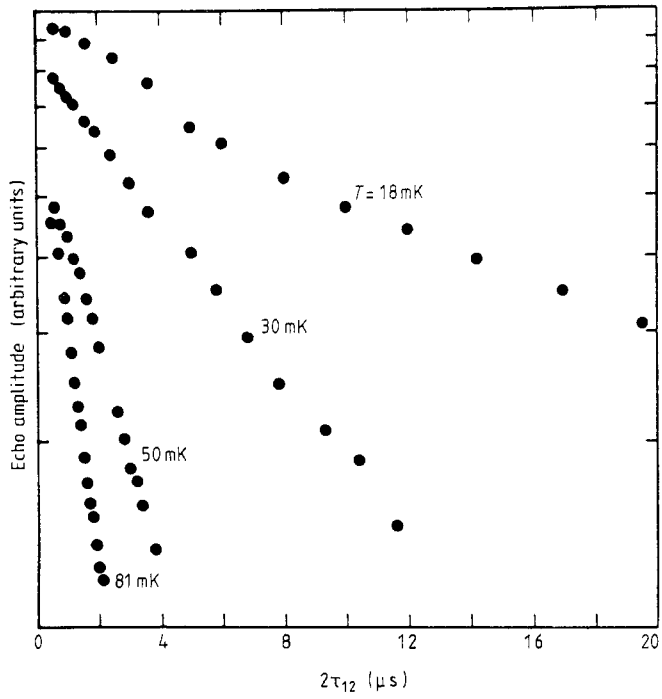

Figure 17. Variation of the spontaneous acoustic echo as a function of pulse separation at a number of temperatures below 100 mK (Golding and Graebner 1981). Suprasil W, $f = 0.692$ GHz.

to maximise the contribution from the intrinsic dipoles. Decay times fitted to the approximately exponential variation give values for the dephasing time T_2 which decrease with increasing temperature as T^{-2}, from a value of 16 μs at the lowest temperature of 18 mK. Similar results were obtained for electric echoes (Golding *et al* 1979) also probing 'intrinsic' TS in silica, but those shown in figure 18 illustrate the

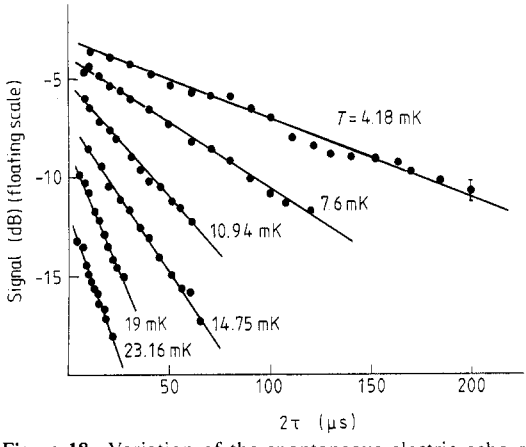

Figure 18. Variation of the spontaneous electric echo amplitude as a function of pulse separation (Bernard *et al* 1979). $P_{in} = -43/40$ dBm.

sensitivity of these echo measurements to the precise experimental conditions. In this set of experiments the strength of the electric field was lower, to probe the OH-related dipoles (Bernard *et al* 1979), but the time constants of the exponential decays vary as T^{-1}, and at 20 mK take the value 40 μs. The microscopic origins of the dephasing time T_2 are discussed in § 5.3.

Experiments to measure the energy relaxation time T_1 require three pulses but for the usual stimulated echo (Black and Halperin 1977) the results give a complicated combination of T_1 and T_2. A more direct measure of T_1 is obtained by using an initial π pulse, followed a time t_0 later by closely spaced $\pi/2$ and π pulses (as for spontaneous echoes). It is important, for reasons that are explained in § 5.3, that the initial pulse is significantly shorter (and therefore of higher intensity) than the succeeding two. If this condition is satisfied the second and third pulses probe TS well within the frequency range excited by the first (remembering $\tau_p \ll T_1, T_2$). The initial π pulse takes the TS from the ground state ψ_1 to the state ψ_2. During the time t_0 a fraction $\exp(-t_0/T_1)$ of the systems will relax back to the state ψ_1. The double-pulse sequence gives a spontaneous echo as before, but the contribution of those systems which decayed back to ψ_1 will be opposed by those remaining in ψ_2. The echo amplitude, independent of any dephasing processes, is equal to the sum of $\exp(-t_0/T_1)$ from ψ_1 and $-[1-\exp(-t_0/T_1)]$ from ψ_1 or $-[1-2\exp(-t_0/T_1)]$. Measurements on silica (Golding *et al* 1979, Bernard *et al* 1979) show that this simple exponential relaxation is not obeyed for larger values of t_0, indicating as expected from § 2.2 a distribution of relaxation times (figure 19). The minimum value measured at short times is in good agreement with (2.26) (Bernard *et al* 1979) with values of γ_L^2 and γ_T^2 close to but slightly larger than those deduced from the variation of spontaneous echo amplitude with acoustic intensity.

One further ingenious electric echo experiment deserves mention. Bernard *et al* (1978) applied a DC electric field pulse between the two oscillating field pulses in a spontaneous echo experiment. The effect of this field is to change the energies of states ψ_1 and ψ_2 so that an additional phase difference of $2\xi p\tau_0/\hbar$ is introduced in (5.6),

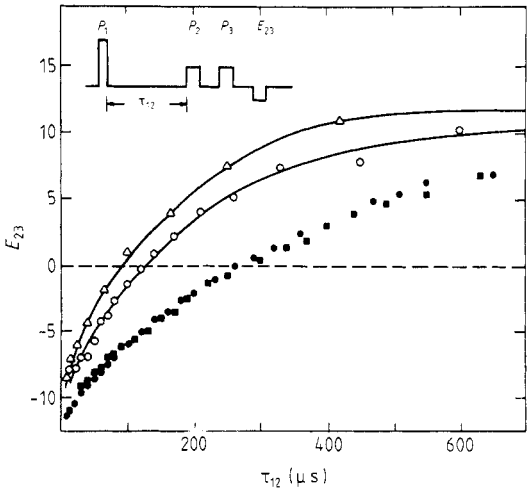

Figure 19. The amplitude of the stimulated electric echo in vitreous silica as a function of the time between the first and second pulses (Golding *et al* 1979). $T = 19$ mK, $f = 0.72$ GHz. △, Infrasil; ○, Herasil; ■, Herasil – OH; ●, Suprasil I – OH.

where τ_0 is the length of the DC pulse, ξ the electric field strength and p the component of the static dipole moment along the field direction. For a given TS this gives an additional factor in the echo of $\cos(2\xi p\tau_0/\hbar)$, because the phase factor is not compensated in the time interval $t_0 < t < 2t_0$, and so the total resultant is

$$E(\xi, \tau_0) = E_0 \int_{-\infty}^{\infty} n_Z(p) \cos(2\xi p\tau_0/\hbar)\, dp \tag{5.9}$$

where $n_Z(p)\, dp$ is the number of TS with component moment p, weighted according to their contribution to the echo. Measurements of $E(\xi, \tau_0)$ as a function of τ_0 (or ξ) give the Fourier transform of $n_Z(p)$. Results indicate an exponential dependence of $E(\xi, \tau_0)$ on τ_0 and hence a Lorentzian distribution function for $n_Z(p)$, but this experiment has not been analysed in detail with inclusion of all weighting factors.

5.3. Spectral diffusion

The short dephasing time T_2 is the result of interactions between tunnelling states. In principle an interaction between two TS with the same energy could take place by mutual excitation and de-excitation with exchange of a resonant phonon (through the term in σ_x in the interaction Hamiltonian (2.15)). In a glass, however, the density of mutually resonant TS is too small for this to be an effective dephasing process. Much more effective is the non-resonant process (involving σ_z) in which a transition of one TS, equivalent to the reorientation of an elastic dipole, gives rise to a change in the strain field experienced by a neighbour, and hence to an energy change. Because all TS with energy less than about $2\, k_B T$ undergo transitions at temperature T, a given state interacts with many more neighbours than is the case for resonant interaction.

A detailed quantitative calculation of T_2 is complicated (Klauder and Anderson 1962, Hu and Walker 1977, Laikhtman 1985), but the following semiquantitive explanation contains the essential physical features. Each TS experiences a fluctuating local strain field which in the steady state gives rise to energy fluctuations of magnitude ΔE_0. In an echo experiment the initial field pulse, of duration much less than the time scale of the fluctuations, selects from the distribution of TS a subset which instantaneously have energy $E_0 = \hbar\omega_0$ (figure 20(b)). Because the mean energies of TS within this subset are different, the energies of the excited systems gradually spread out over an energy range ΔE_0, as shown in figure 20(b). At times long compared to the time scale

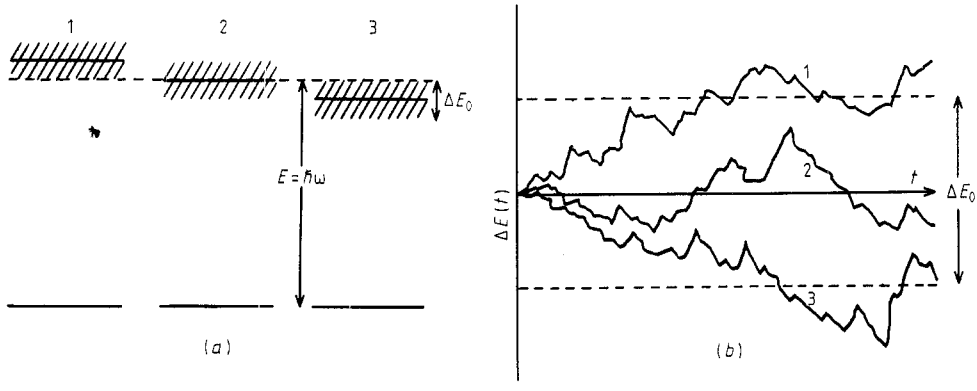

Figure 20. A schematic representation of the way in which spectral diffusion leads to an increase in linewidth with time.

of the fluctuations, governed by the average energy relaxation time T_1, the width of the energy distribution of the subset reaches ΔE_0, and is then independent of time. However, the most interesting physical aspects of the interaction involve the time variation of this width $\Delta E(t)$.

The magnitude of ΔE_0 can be evaluated from the strength of the coupling between TS and phonons. Ignoring the tensorial character of the strain field (Black and Halperin 1977), the interaction energy between a pair i, j of TS separated by distance r_{ij} can be written

$$\delta E = C\frac{\gamma_i\gamma_j}{\rho v^2 r_{ij}^3}\frac{\Delta_i\Delta_j}{E_iE_j} \tag{5.10}$$

where $\gamma_i\Delta_i/E_i$ and $\gamma_j\Delta_j/E_j$ are the static elastic dipole moments and C is a constant of order unity. Replacing $1/r_{ij}^3$ by the concentration of thermally excitable TS, Pk_BT, and averaging over neighbours j gives

$$\Delta E_0 = C\frac{\gamma^2 Pk_BT}{\rho v^2}\frac{\Delta}{E} \tag{5.11}$$

for a state of asymmetry Δ. The factor Δ/E is included to show explicitly that the interaction energy which determines T_2 is correlated with the induced dipole moment given by $\gamma\Delta_0/E$, but will be ignored in the remainder of the analysis.

The effect of this 'spectral diffusion', in which the excitation is spread out over an energy range ΔE_0, is dependent on the time interval t_0 between the two pulses in the spontaneous echo experiment. In the long time limit $t_0 \gg \tau_{\min}$ where $\tau_{\min}$ is defined as the shortest energy relaxation time for TS with $E \sim k_BT$ and is given by (2.26) with $E = \Delta_0 = k_BT$, T_2 is the time for which the spread in phase $\Delta E_0 t/h$ is of order $\pi/2$. This condition gives

$$T_2^{-1} = \frac{\pi}{2}\frac{\Delta E_0}{\hbar} = \frac{C\pi P\gamma^2 k_BT}{2\hbar\rho v^2}. \tag{5.12}$$

Because the phase difference increases with t the echo decay is essentially exponential for $t_0 \gg \tau_{\min}$, with T_2 inversely proportional to T.

At short times, $t_0 \ll \tau_{\min}$, the width of the energy distribution $\Delta E(t)$ increases approximately as $\Delta E_0[1-\exp(-t/\tau_{\min})]$, so that

$$\Delta E(t) \simeq \Delta E_0 t/\tau_{\min}. \tag{5.13}$$

The dephasing time is given by the condition

$$\frac{1}{\hbar}\int_0^{T_2}\Delta E(t)\,\mathrm{d}t = \frac{\pi}{2} \tag{5.14}$$

leading to

$$T_2^2 = \hbar\pi\tau_{\min}/\Delta E_0. \tag{5.15}$$

The decay is non-exponential, varying with t_0 as

$$\exp(-\Delta E_0 t_0^2/\hbar\tau_{\min}). \tag{5.16}$$

The echo amplitude therefore decays to $1/e$ of its initial amplitude in a time T_2 which varies as T^{-2} for $t_0 \ll \tau_{\min}$, using $\tau_{\min}$ proportional to T^{-3} (§ 4.3).

The extent to which spectral diffusion is observable in a *spontaneous echo experiment* depends on the relative magnitudes of t_0 and $\tau_{\min}$. Using (2.26) and the measurements of T_1 described in the last section, $\tau_{\min}$ can be estimated as 100 μs at 20 mK in silica.

The condition $t_0 \ll \tau_{min}$ is therefore well satisfied for $t_0 = 10\ \mu$s at 20 mK, and the results for the lowest temperature shown in figure 17 for 'intrinsic' phonon echoes should demonstrate spectral diffusion. The dependence of echo amplitude on t_0 is however more nearly exponential than Gaussian, although T_2 varies as T^{-2} and the value of 10 μs calculated from (5.15) is in agreement with the measured value. Results for electric echoes from intrinsic TS in silica also give the same value for T_2 at 20 mK, although the decay is again non-Gaussian but with T_2 varying as T^{-1}.

There seems no obvious explanation for this discrepancy, although it may be a result of the extreme sensitivity of the results to experimental conditions consequential on the broad distribution of TS parameters. In particular, the pulses probe states of energy $E = \hbar\omega$ but with a range of Δ and hence a range of interaction energies ΔE_0 (5.11). The resultant decay will therefore be a superposition of terms of the form given by (5.16). Smaller values of ΔE_0 give a slower decrease of echo amplitude which at long times can make the decay approximate to an exponential instead of a Gaussian form. However, the shape depends significantly on the precise tuning condition, and a critical assessment of data is difficult on the basis of published information.

Spectral diffusion involving TS is also important in controlling the *homogeneous linewidth* (equal to $\hbar/T_2$) of optically active impurities in solids. In these experiments the energy $\hbar\omega_0$ of the relaxing species is very much greater than $k_B T$, in contrast to TS echo experiments where the two are comparable. Examples include Nd^{3+} in SiO_2 where T_2 was measured by a photon echo experiment (Hagarty *et al* 1982), and organic glasses (Thijssen *et al* 1982) where the linewidth was measured by photochemical hole burning. Values of T_2 fall in the range $10\ \text{ns} < t_0 < 1\ \mu$s at 1 K, but all decrease with increasing temperature as $T^{-1.3}$ in the range $0.1 < T < 10$ K. Three separate publications (Lyo 1981, Hunklinger and Schmidt 1984, Huber *et al* 1984) have contained explanations based on spectral diffusions, all in essence giving the arguments presented above albeit in slightly different forms. The only significant difference is the extension to more general forms of interaction, replacing (5.10) by a potential varying as $1/r^m$, and by the inclusion of higher-order phonon processes in determining τ_{min} above 1 K.

The experiments are carried out in the long-time regime, so that T_2 is given by (5.12) in contrast to the TS echo experiments. This difference may also justify the inclusion of an energy dependence of P in the optical experiments to give the observed temperature dependence of $T^{-1.3}$, while ignoring it for TS echoes. In fact Hunklinger and Schmidt (1984) derived the additional $T^{0.3}$ factor by the dependence of the effective density of states on time, as in the discussion of § 3.1.

The analysis of *saturation in pulse experiments* (§ 4.2) is complicated by spectral diffusion. In an experiment where the width of the 'hole' burnt into the TS distribution by the saturating pulse is constant with time, a measure of the attenuation of a second weaker pulse as a function of the time separation between the pulses allows measurement of T_1. The extent to which this ideal arrangement can be realised in practice depends on the relative magnitudes of τ_p the pulse length, T_1 and T_2 for the TS of energy $\hbar\omega_0$, and τ_{min}, the characteristic minimum relaxation time for neighbouring states which determines the time scale of spectral diffusion. If $\hbar\omega_0 < k_B T$ then $\tau_{min} < T_1$ and vice versa. Different regimes may be classified as follows.

(i) $\tau_p < T_1, T_2$. The hole burnt into the TS distribution has a width $\hbar/\tau_p$, larger than that produced by spectral diffusion, which will therefore not be important. T_1 is measured.

(ii) $T_2 < \tau_p < T_1$. Under these conditions spectral diffusion may be important because the hole in the distribution can broaden and become shallower with time

following the initial pulse. Only if $\tau_p < \tau_{min}$ is this a major factor, because otherwise spectral diffusion during the pulse will allow saturation of a hole of width $\hbar/T_2$, and subsequent spectral diffusion will have little effect. Difficulties of interpretation may occur if $\hbar\omega_0/k_BT$ is not much less than unity.

(iii) $\tau_p > T_2, T_1$. In this steady state regime spectral diffusion is only important if $\hbar\omega_0/k_BT \gg 1$, unlikely at high temperatures where relaxation times are short.

The most straightforward results to interpret are those for which $\tau_p \sim T_2$ or less, as was the case for those shown in figure 21 (Golding and Graebner 1981). Although the attenuation recovery is not an exponential function of pulse separation, the asymptotic behaviour at small times defines a relaxation time which is in good agreement with that calculated for a one-phonon process (2.26) with $\gamma = 1.5$ eV. The slower recovery at longer times may reflect the broad distribution of TS relaxation times.

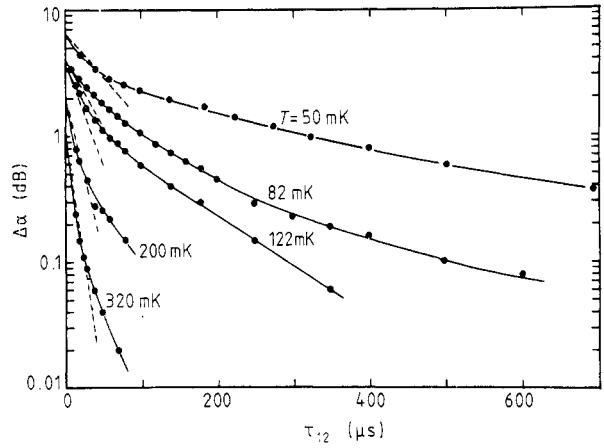

Figure 21. The change in attenuation of a weak probing pulse applied a time τ_{12} after a saturating pulse (Golding and Graebner 1981). Suprasil W, $f = 0.692$ GHz, $L = 0.635$ cm.

One further experimental feature can complicate the interpretation of saturation recovery experiments. It is convenient for experimental reasons to observe the recovery using a second pulse which is not weak (Hunklinger and Arnold 1976). Consequently the relationship between attenuation and occupation probabilities is non-linear. Hunklinger and Arnold (1976) used the steady-state solutions of the Bloch equations (4.15)-(4.17) to relate the two, but it is difficult to ensure that the necessary condition $\tau_p \gg T_1$ is indeed valid.

Direct observation of spectral diffusion is possible by using an intense saturating pulse of variable frequency ω followed by a weak pulse of fixed frequency ω_0. (It is obviously more convenient to fix the frequency of the weak pulse, although in practice even the probing pulses are sufficiently intense to be affected by saturation.) By measuring the attenuation of the second pulse as a function of ω at a fixed and very short time interval between pulses, the linewidth can be measured directly. Experimental results at 0.4 K in silica (Arnold *et al* 1978) show not only a linewidth much greater than $\hbar/\tau_p$ or $\hbar/T_1$, but an increase in linewidth with increasing pulse length, giving direct evidence for spectral diffusion (figure 22). The results are in good agreement with calculations based on the physical ideas leading to (5.15) and (5.16) (Black and Halperin 1977).

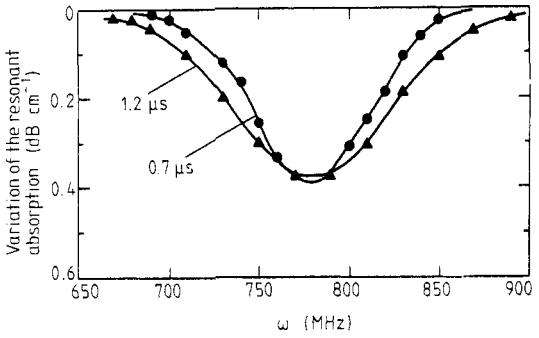

Figure 22. Attenuation of a probing pulse of fixed frequency as a function of the frequency of a saturating pulse for two different values of saturating pulse length (Arnold *et al* 1978). Vitreous silica, $T = 0.42$ K.

Measurements at fixed time interval in a borosilicate glass BK7 have been collected together in figure 23 (Graebner and Golding 1981). Experimental values of the linewidth $\Delta\omega$ are compared to the predictions of a spectral diffusion model, showing that $\Delta\omega$ is proportional to T^4 at low temperatures where the short time limit (5.16) applies. (The calculated curve in figure 23 is for a pulse separation of 1 μs, a reasonable approximation for simultaneous 1 μs pulses and for shorter pulses with 1 μs separation). At high temperatures $\Delta\omega$ is given by $\Delta E_0/\hbar$ from (5.12) in the limit $\tau_{\min} \ll 1$ μs. The agreement between theory and experiment gives further strong support for spectral diffusion as a dominant contribution to T_2.

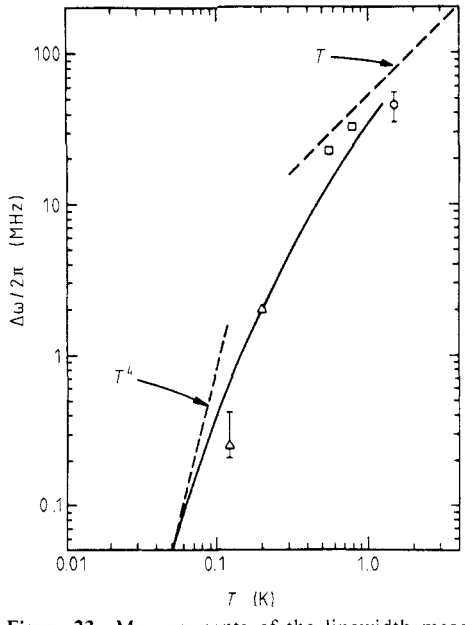

Figure 23. Measurements of the linewidth measured at different frequencies and temperatures in a borosilicate glass BK7 (Golding and Graebner 1981). The full curve is calculated from a spectral diffusion model. △, 0.692 GHz; □, 0.738 GHz; ○, 8.9 GHz.

6. Metallic glasses

There have been a number of recent review articles on the low-temperature properties of amorphous metals, (Black 1981, Lohneysen 1981, Hunklinger and Raychaudhuri 1985) and so this section will be limited to a survey of the way in which the interaction between TS and electrons modifies the results described in the previous sections. There have been detailed theoretical examinations of the coupled electron TS problem based on analogies with the Kondo problem, but in general the only well established experimental consequence of the interaction is the greatly reduced relaxation time of the TS.

The interaction between electrons and TS is represented formally by a Hamiltonian H_2 of the form (Golding *et al* 1978, Black *et al* 1979)

$$H_2 = \sum_{kk'} (\Delta_0/E) K\sigma J_x C_{k'}^{+} C_k \tag{6.1}$$

in spin notation, where $C_{k'}^{+}$ and C_k are electron operators. An electron in state k is scattered into state k' with loss of energy E transferred to the tunnelling state (or vice versa). Normally k and k' define the momentum of the electrons represented as plane waves, but are used here simply as labels in view of the fact that the random structure of amorphous metals invalidates the concept of a well defined electron momentum. The Hamiltonian assumes that the spatial extent of each TS is smaller than the inelastic electron scattering length. K is the TS-electron coupling constant.

Following § 2.2 the TS relaxation time can be calculated from the transition probabilities ω_{12} and ω_{21}, where ω_{12}, for example, is given by

$$\omega_{12} = \frac{2\pi}{\hbar} \sum_{kk'} |\langle \psi_1 | H_2 | \psi_2 \rangle|^2 f_k (1 - f_{k'}) \delta(E - \varepsilon_{k'} + \varepsilon_k). \tag{6.2}$$

The Fermi function f_k represents the probability of finding state k occupied. Replacing the summation in (6.2) by an integral

$$\omega_{12} = \frac{2\pi}{\hbar} \frac{K^2}{2} \int_0^\infty n(\varepsilon_{k'}) n(\varepsilon_k) f_k (1 - f_{k'}) \frac{\Delta_0^2}{E^2} \delta(E - \varepsilon_{k'} + \varepsilon_k) \, \mathrm{d}\varepsilon_k \, \mathrm{d}\varepsilon_{k'}$$

where a factor of $\frac{1}{2}$ arises from electron-spin conservation if $n(\varepsilon_k)$ is the total electron density of states at energy ε_k. The major contribution comes from states close to the Fermi level, so that on integration

$$\omega_{12} = \frac{\pi}{\hbar} [n(\varepsilon_F) K]^2 (\Delta_0/E)^2 E [1 - \exp(-E/k_B T)]^{-1}.$$

Combining with a similar expression for ω_{21} gives

$$T_1^{-1} = \frac{\pi}{\hbar} (n(\varepsilon_F) K)^2 (\Delta_0/E)^2 E \coth(E/2k_B T). \tag{6.3}$$

The strength of the electron-TS interaction can be gauged from the upper limit on T_1 imposed by saturation recovery experiments (§ 5). A large intensity saturating pulse has no measurable effect on the propagation of a second weak pulse even for pulse separations as short as 100 ns (Golding *et al* 1978). An upper limit of 25 ns for T_1 at 10 mK should be compared with the values of approximately 200 μs for T_1 and 50 μs for T_2 in silica at the same temperature (§ 5.2).

In metallic glasses the electron interaction determines both T_1 and T_2 at low temperatures with $T_1(\min) \equiv \tau_{\min}$ varying as T^{-1}. As the temperature is raised, the phonon-TS interaction becomes relatively more important, dominating above a few degrees K (in much the same way as the phonon heat capacity dominates the electronic contribution) and giving $\tau_{\min}$ proportional to T^{-3}. The lifetime broadening of the TS levels is significantly increased, but because of the already broad distribution of energies in general this is expected to have little effect (Thomas 1983).

Because of the reduced $\tau_{\min}$ relaxation processes are observable at lower temperatures in metallic glasses. Results equivalent to (4.34), (4.35) and (4.36) can be derived by using (6.3). In the limit $\omega\tau_{\min} \gg 1$

$$l^{-1} = \frac{\pi^3}{24}\frac{(P\gamma^2)}{(\rho v^2)}\frac{(n(\varepsilon_F)K)^2}{\hbar v} k_B T \tag{6.4}$$

and the velocity change is negligible. For $\omega\tau_{\min} \ll 1$,

$$l^{-1} = \frac{(P\gamma^2)}{(\rho v^2)}\frac{\pi\omega}{2v} \tag{6.5}$$

as in an insulating glass because the result is independent of the form of the relaxation time, and

$$\frac{\Delta v}{v} = -\frac{1}{2}\frac{(P\gamma^2)}{(\rho v^2)}\ln(T/T_0) \tag{6.6}$$

where the factor of $\frac{3}{2}$ in the insulating glass is replaced by $\frac{1}{2}$. In a metallic glass the condition $\omega\tau_{\min} = 1$ is satisfied for frequencies of the order of 500 MHz at approximately 100 mK, so that the logarithmic slope measured in a velocity experiment below 1 K contains both resonant and relaxation contributions of opposite sign giving a resultant

$$\frac{\Delta v}{v} = +\frac{1}{2}\frac{(P\gamma^2)}{(\rho v^2)}\ln(T/T_0). \tag{6.7}$$

The combination of the two contributions to the attenuation is additive ((3.4) and (4.35)) so that values of γ^2 deduced naively from $\Delta v/v$ using (4.4) give much smaller values than those given by the thermal conductivity or ultrasonic attenuation. Detailed fitting of experiments is needed to give good agreement with theory, as shown in figure 24.

At higher temperatures where phonons take over from electrons as the dominant cause of TS relaxation, the velocity variation given by adding (4.4) and (4.37) is negative. In practice higher-order phonon processes modify the logarithmic dependence to give an almost linear decrease of velocity with temperature. However, it should be noted that the maximum in $\Delta v/v$ seen typically at 2-3 K in metallic glasses differs in origin from that seen in insulating glasses. The latter is produced when the resonant increase in $\Delta v/v$ is balanced by the decrease caused by relaxation, and occurs when $\omega\tau_{\min} \sim 1$ at a temperature which scales as $\omega^{1/3}$. In a metallic glass the maximum occurs at a temperature T_m which is almost frequency independent.

The phenomenon of saturation is also complicated by electron-TS interaction. The critical intensity I_c needed to saturate resonance absorption (4.25) is greatly increased in metals because the relaxation times are much smaller. Figure 25 shows attenuation as a function of acoustic intensity in an amorphous metal PdSiCu. Before comparing with the corresponding curve for silica (figure 13) it is important to make sure that resonant scattering dominates at 62 mK and 720 MHz. Because $\omega\tau_{\min} > 1$ for PdSiCu

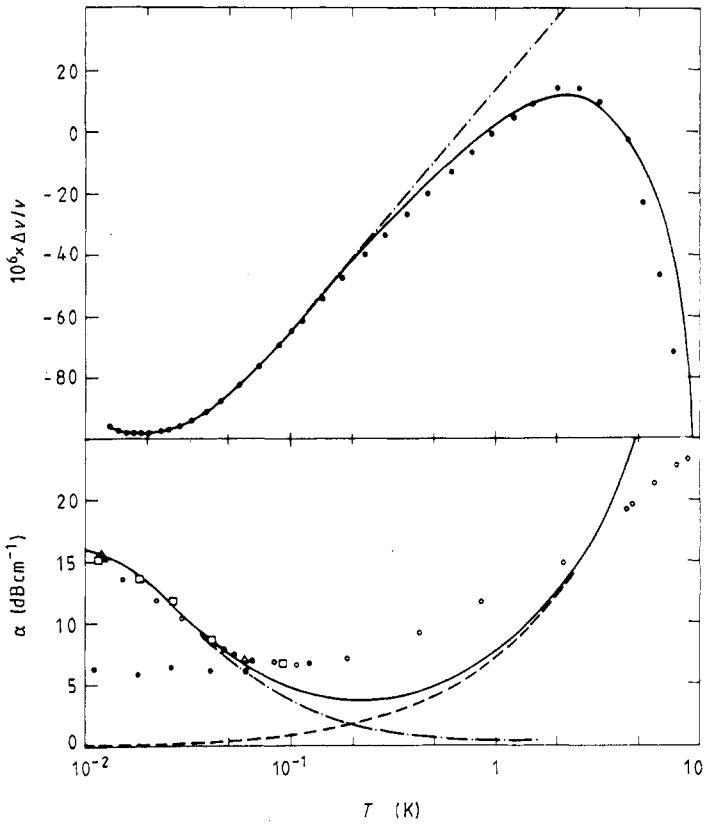

Figure 24. The attenuation and velocity of acoustic waves in the metallic glass PdSiCu as a function of temperature, together with the behaviour expected from the tunnelling model (full curve) (Golding *et al* 1978). $f = 0.96$ GHz.

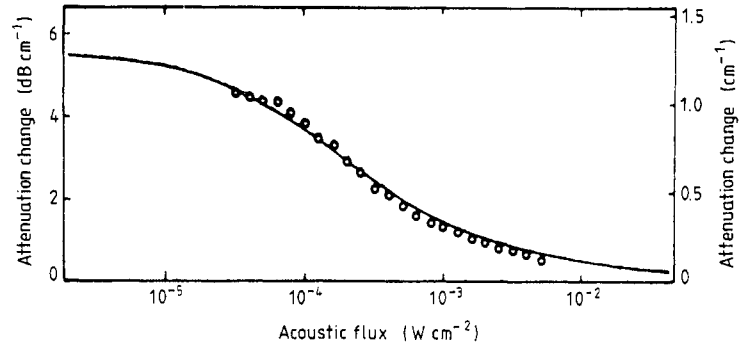

Figure 25. Attenuation as a function of acoustic intensity in amorphous metallic PdSiCu. $T = 0.062$ K, transverse $f = 720$ MHz.

under these conditions, the total attenuation is the sum of resonant and relaxation contributions given by (3.4) and (6.4) respectively. Evaluation of the terms shows that the resonant term is larger by a factor of about 10, and so comparison with the case of silica is indeed valid. As expected I_c is much larger in the metallic glass.

Saturation is also observed when relaxation dominates the attenuation, at low frequencies and temperatures above 100 mK (Araki *et al* 1980, Hikata *et al* 1981). This does not happen in an insulating glass because the intense pulse saturates only those TS within an energy range $\hbar/T_2$ about the exciting frequency, small in comparison with the effective width $k_B T$ of the distribution of states contributing to relaxation. In contrast the very short relaxation times in the metallic glass allow saturation of a significant fraction of the TS contributing to the relaxation. At 0.2 K, for example, T_2, approximately equal to T_1, is about 1 ns, leading to a broadening equivalent to 0.1 K. In practice the effect is enhanced by the power dependence of the linewidth.

Formally this can be taken into account by including the steady state solutions of the Bloch equations in the treatment of relaxation. Strictly speaking, the Bloch equations are not valid in the limit $\omega T_2 \ll 1$ but have been generalised to describe metallic glasses (Continento 1982, Arnold *et al* 1982). The latter paper gives a detailed fit to experiment in PdSiCu showing clearly the relative contribution of resonant and relaxation terms, and demonstrating that both can be saturated.

The fact that a range of TS energies comparable to $k_B T$ can be saturated by a single pulse suggests that acoustic velocity is also a function of acoustic power in metallic glasses. An increase of velocity with increasing power has indeed been observed in PdSi (Cordié and Bellessa 1981) and explained on the same basis as the power dependence of relaxation attentuation. The data allow a determination of T_2, approximately 2 ns at 10 mK in agreement with experiment.

The effect of electrons in determining T_1 for TS in amorphous metals is dramatically confirmed by acoustic measurements in amorphous superconductors. Below the transition temperature T_c the number of effective electrons decreases with decreasing temperature, leading to an increase in T_1 (Black and Fulde 1979). There is a close parallel between the behaviour of T_1^{-1} and ultrasonic attenuation in (crystalline) superconductors, both reduced from the normal state value by a factor $f(\Delta_s/kT)$, where f is the Fermi factor and Δ_s the superconducting energy gap, in the limit where the TS or phonon energy is small compared to Δ_s.

The behaviour of the acoustic attenuation in an amorphous superconductor depends critically on the relationship between T_c and T_m the temperature at which resonant and relaxation contributions are equal, and on the value of $\omega\tau_{min}$ at T_c. For the results shown in figure 26, $T_c > T_m$ and $\omega\tau_{min} \ll 1$ at T_c. The attenuation is dominated by relaxation, which in the limit $\omega\tau_{min} \ll 1$ is, from (6.5), insensitive to the form of τ_{min} and proportional to ω, as observed (Arnold *et al* 1981). Nothing happens at T_c because the TS-phonon interaction dominates, but at lower temperatures the attenuation falls more rapidly in the superconducting than in the normal state. In the normal state the electron-TS interaction becomes more important than the phonon-TS contribution at about 1 K, but because the condition $\omega\tau_{min} \ll 1$ is still satisfied, the attenuation does not change. By contrast, in the superconductor where both the electron and phonon interactions are decreasing rapidly with temperature, $\omega\tau_{min}$ increases and the attenuation is now (from (4.36)) dependent on the form of T_1. Below about $T_c/2$ the attenuation decreases as T^3, characteristic of a one-phonon process.

Although these ideas explain the main features of the results the picture is not yet complete. Measurements below 1 kHz in $Cu_{30}Zr_{70}$ and $Pd_{30}Zr_{70}$ show a large increase

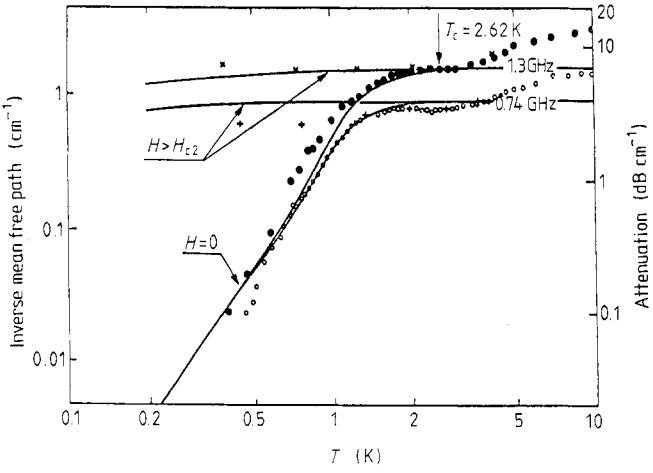

Figure 26. Attenuation as a function of temperature in the amorphous superconductor $Pd_{30}Zr_{70}$ (Arnold *et al* 1981). Longitudinal waves: ——, theory; ○, ●, ×, +, experiment.

in attenuation well below T_c (Esquinazi *et al* 1986). The difference is consistent with an increase in $P\gamma^2$ in the superconducting state, and is presumably observed clearly at low frequencies because the condition $\omega\tau_{min} \ll 1$ is valid to lower temperatures.

7. Microscopic descriptions of tunnelling states

In a limited general review of this kind a detailed survey of specific microscopic models is impossible and it is more appropriate to illustrate approaches to a microscopic description of TS by means of well chosen examples. Generally models for tunnelling states have been considered in three distinct categories: by relating tunnelling states to established defects in amorphous or crystalline materials, by computer modelling and thirdly as a consequence of general (and often imprecise) theories of the glassy state. Each of these will be considered in turn, but only theories relating specifically to TS are included.

7.1. Relation to specific defects

The earliest and still one of the more convincing descriptions of a tunnelling state is based on measurements in a mixed phase metallic NbZr crystalline alloy (Lou 1976). The material is disordered because it contains small regions of one phase (ω) in a matrix of another (β). For example, in $Nb_{20}Zr_{80}$ the isolated regions of ω phase are typically 0.5 nm in diameter, and are formed by suitable heat treatment at a concentration of about 10^{25} m^{-3}. Measurements of the heat capacity and thermal conductivity show 'glassy' behaviour, dependent on the concentration of ω phase. Microscopically the tunnelling states in this case can be identified with the atomic displacements occurring in the β-ω phase transition (figure 27) in which two atoms move simultaneously through a distance of about 0.05 nm. Lou (1976) argues that this configurational change can be described by a double-well potential, and presents experimental evidence to support the existence of a wide range of barriers. Such a microscopic state is of exactly the form suggested by the tunnelling model and could undoubtedly exist in true glassy metals.

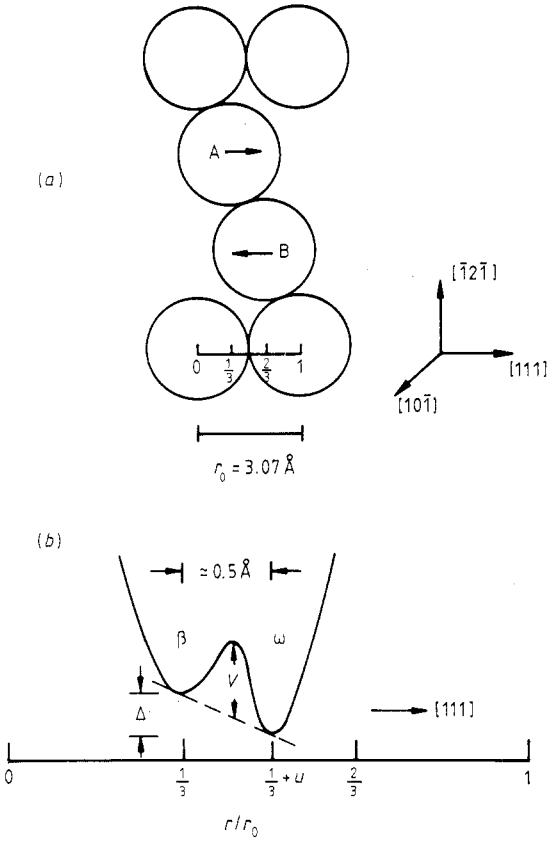

Figure 27. Atomic displacements and the local potential barrier involved in the β-ω phase transition in NbZr (Lou 1976).

Another known impurity, water, has been identified as a tunnelling state in vitreous silica. Existing in the form of hydroxyl ions, it couples strongly to electric fields and can be readily studied through measurements of the dielectric constant (§ 4.1) or in electric echo experiments (§ 5.2). This particular impurity can be analysed in detail because the geometry of the displacement is established, and the density of states depends only on the distribution of barriers (V_0 in (2.5)). Using a distribution of V_0 derived from higher-temperature dielectric measurements, the effect of OH on the thermal and dielectric properties below 1 K can be understood in quantitative detail (Phillips 1981c).

An interesting connection has been made between tunnelling states and the states important in the optical and electrical properties of chalcogenide (and oxide) glasses, with particular reference to As_2S_3. These glasses show an activated conductivity and no electron spin resonance signal as normally prepared, implying an absence of unpaired electrons in contrast, for example, to pure amorphous germanium.

These and other experimental results were brought together and explained by Street and Mott (1976) using a model based on a spin pairing idea of Anderson (1975) which demonstrated the consequences of a strong attractive interaction between an electron and its surroundings. The energy of each electron can be reduced by local distortion, even to the extent of allowing two electrons to occupy the same site if the decrease in

individual electron energy more than compensates for the repulsive Coulomb interaction between the two electrons. This pairing of electrons into 'bipolaron' or D^- states (Street and Mott 1976) explains why no free spins are observed in chalcogenide glasses, although it must be pointed out that no detailed microscopic justification has yet been achieved. However, support for the model is provided by the fact that it can explain the large difference in frequency between absorbed and emitted light in luminescence experiments, and the photoexcitation of free spins. A spin resonance signal can be induced by irradiation with photons of energy slightly less than the band gap, and destroyed by annealing or by irradiation with infrared light of about half the inducing energy.

These paired electron 'defects' are mobile, but can move only between sites separated by no more than one or two atoms (Phillips 1976, Elliott 1979, Licciardello *et al* 1981, Karpov 1985) so that there is significant overlap between local distortions on the two sites. This mobility gives rise to AC conductivity (Elliott 1979, Long 1982) and also to the possibility that these defects can contribute to the low-temperature heat capacity (Anderson 1975) both in chalcogenide glasses and in SiO_2 (Russo and Ferrari 1984). It is clear that for small site separation there is no clear theoretical distinction between the motion of electrons accompanied by local displacements of ions and the atomic motion proposed in the tunnelling model.

On the experimental side there is clear evidence of a close connection between these defects and tunnelling states. Fox *et al* (1982) show that the low-temperature photon echo signal in As_2S_3 is sensitive to bandgap light, decreasing on irradiation. Conversely the signal increases on annealing and under illumination with intense infrared light, and so behaving in a way expected for paired electrons. The implication of these experiments is that paired-electron defects behave as TS at low temperatures.

It is not possible to state the converse, that TS are the same as paired electron states, because careful analysis of the experiment suggests that the density of optically sensitive TS is much less than the total density of TS (Phillips 1985a). The fact that the dielectric constant (§ 4.1) is insensitive to light indicates that the echo experiments probe only a small proportion of TS with large dipole moments (§ 5.2). This is not altogether surprising, because the density of states deduced from heat capacity data in As_2S_3 is known to be much greater than that obtained from AC conductivity, and perhaps the most interesting feature of the experiments is confirmation that the tunnelling picture is a very general one. At sufficiently low temperatures any almost degenerate coupled localised states will, in the random environment provided by a glass or otherwise disordered solid, give rise to properties describable by the tunnelling model.

7.2. Microscopic modelling

Random-network models of amorphous structures have been extremely useful in providing atomic coordinates for the calculation of a wide range of physical properties. Most structural calculations use as a starting point physically constructed models which are subject to straightforward rules imposed by atomic coordination and limited variations in bond length and angle (Etherington *et al* 1982). These constructions are subsequently 'relaxed' by computer to minimise the energy, usually using a form of interatomic potential described by Keating (1966). The success of this approach has led to attempts to search structural models in order to discover double-well potentials or locally metastable states, although in general the models have been constructed

from the outset by computer simulation, in order to avoid the constraints inherent in physical modelling.

Smith (1978) started with a random arrangement of 250 atoms (subject to periodic boundary conditions to avoid surface effects) and, by moving each atom in turn, minimised an interatomic potential energy which included spherically symmetric long-range attractive and core repulsive terms, together with an additional term which was a minimum for tetrahedral coordination. The resulting model gave reasonable agreement with experimental radial distribution functions, although the variation of bond angles was greater than that found when starting from physically constructed models.

The most interesting feature of the results appeared in a search of local potentials, carried out by calculating the energy of each atom in turn as it was displaced by finite amounts from its equilibrium position. Approximately four local minima per atom were found, although for the vast majority the additional energy in the second minimum was much larger than the bond energy. The distribution of barriers also extends out to similarly large energies, but the calculation appears to show that there are sufficient states of low asymmetry and sufficiently small barriers to be interpreted as TS.

Wooten and Weaire (1984) show that by interchanging sufficient bonds in crystalline Ge the resulting disordered Ge does not revert to the crystal on subsequent energy relaxation, but gives a structure similar to that expected for the amorphous form. This model can be 'searched' for single-atom double-well potentials, and as before the calculation indicates a finite density of the resulting TS, although the range of asymmetry is much less.

Two basic problems complicate the significance of this work on Ge. The first is that the experimental evidence for TS in idealised amorphous Ge (i.e. a continuous random network) is not clear, the available measurements showing a decrease in the TS density of states as the physical density increases towards the ideal value (Duquesne and Bellessa 1983, Löhneysen and Schink 1982, Graebner and Allen 1984, Phillips 1985b). Secondly, and this problem is not restricted to Ge, a search for double minima in which only one atom is moved at a time is not an adequate representation of the real atomic motion, and will seriously overestimate barrier heights. This second point is not easily overcome, and indeed is an example of a general problem of optimisation.

A related approach has been described by Brawer (1981), who used a molecular dynamics calculation with completely spherically symmetric potentials as a representation of the relatively ionic BeF_2. The main conclusion of this work is that defects in the form of threehold coordinated Be and F ions can be quenched into the glass (on a very rapid timescale), and that these defects result in local motion which is compatible with that needed to form TS. It is doubtful, however, that spherically symmetric potentials allow glass formation on a laboratory timescale.

Guttman and Rahman (1985) adopted a slightly different approach in which they studied very-low-frequency modes in a relaxed structure of SiO_2 in order to give a microscopic description of TS. Using the eigenvectors as a guide to the cooperative motion involved at very low frequencies, the potential energy was calculated as a function of displacement in configurational space, a combination of a large number of individual atom displacements. A double-well potential was observed, corresponding to the correlated displacement of about 10 (at least) SiO_4 tetrahedra, although the barrier was very small. This approach is interesting in that it automatically involves cooperative motion, and is consistent with low-frequency inelastic neutron scattering experiments (Buchenau *et al* 1984, 1986) which indicate similar local motion (figure 28). However, values of energy barriers and displacements are likely to depend critically

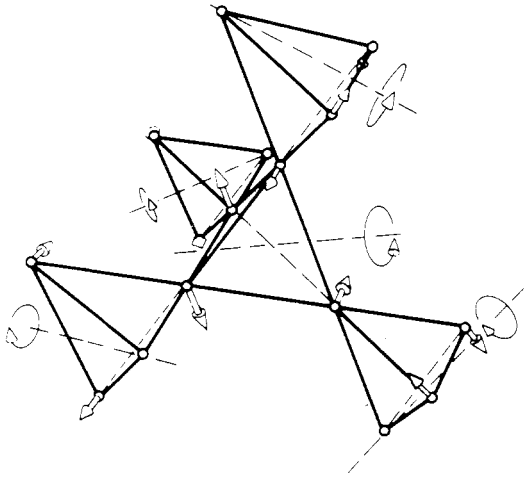

Figure 28. Coupled rotation of SiO_4 tetrahedra as deduced from low-frequency inelastic neutron experiments (Buchenau *et al* 1984).

on the particular choice of force constants. Calculated eigenvectors are particularly sensitive to this choice.

7.3. General theories

In contrast to the more specific approaches described in §§ 7.1 and 7.2, there have been a number of theories which introduce TS as a consequence of a general discription of the glassy state or of the glass transition. As a result of their generality it is often difficult to derive even semiquantitative parameters from these theories, although several qualitative predictions agree with experiment. However, the universal occurrence of TS in disordered solids suggests a basic connection with structure, although it must be emphasised that TS are not restricted to glasses. It may well be that variations in local environment resulting from any kind of disorder are sufficient to give the behaviour described in this review.

The relationship between physical properties and the 'rigidity' of an amorphous network has been examined in some detail in germanium selenide glasses by considering constraints acting on the system. Atoms in a network where bond lengths and bond angles take (ideally) fixed values are subject to constraints; each constant bond length and independent bond angle gives a relation between coordinates of neighbouring atoms. An m-fold coordinated atom provides $m/2$ constraints to the network from constant bond lengths, and $2m$-3 from constant bond angles. Applied to Ge_xSe_{1-x} this gives an average of $5x+2$ constraints per atom, and hence to a critical composition of $x = 0.2$ where the total number of constraints per atom just balances the three degrees to freedom.

This critical composition marks a boundary between underconstrained 'floppy' glasses for $x < 0.2$, and overconstrained glasses with unrelieved strain energy. The strain energy will increase with x, so that it is not surprising to find that bulk glasses cannot be prepared for $x > 0.42$. For $0.2 < x < 0.42$ the model has been used as a basis for claims that the random network model is inadequate (Phillips 1979), and that glasses in this range of composition are built up from tightly coordinated clusters held together by much looser bonding.

Thorpe (1983) has linked the number of tunnelling states to the number f of unconstrained degrees of freedom. In the simplest approximation $f = 1 - 5x$ but in practice the approach to zero is likely to be smoother than this. Qualitatively the model predicts that the density of TS should *decrease* as x increases, becoming vanishingly small for $x > 0.3$. A contrasting approach was taken by Phillips (1981), who associated TS with chalcogenide atoms on the surfaces of the clusters for $x > 0.2$. In this case the number of TS should *increase* with x.

Ultrasonic velocity measurements (§ 4.1) in Ge_xSe_{1-x} show a logarithmic temperature dependence which indicates that $P\gamma^2$ decreases as x increases (Duquesne and Bellessa 1985) and, less directly, that γ is almost independent of x. This behaviour supports the idea that TS are related to the unconstrained degrees of freedom f, although agreement is only qualitative.

Other attempts have been made to associate TS with particular aspects of the glassy state. Mon and Ashcroft (1977) point out that diffraction studies in glasses commonly show a split second peak in the radial distribution function, indicating two possible next-nearest-neighbour configurations. From this they conclude that TS are a subgroup of these configurations in which a number of atoms can move from one to the other, although as mentioned earlier no realistic estimate of barrier potentials is possible. Applied to SiO_4 tetrahedra in silica this idea resembles an earlier one due to Vukcevich (1972). For completeness an abstract theory based on the lack of range order in certain glasses should also be mentioned (Duffy and Rivier 1983), as should a generalised theory of local anharmonic potentials (Karpov *et al* 1983).

A second group of general theories is based on the observation that the density of TS decreases as the glass-transition temperature T_g increases from one glass to another (see, for example, Hunklinger and Raychaudhuri 1986). Although this result follows generally from the arguments given in § 2.1, a recent formulation of the well established free-volume theory of the glass transition by Cohen and Grest (1980, 1981) has given a correct order-of-magnitude estimate of the density of TS. They point out that the number of TS depends on the ratio of molecular volume to the free volume which is frozen into the glassy state at T_g. Moreover, the same parameter determines the viscosity of the supercooled liquid at the glass transition, usually defined to occur when the viscosity reaches a particular value. This means that the basic parameter of the theory is determined by T_g, and so all materials should have a similar total number of TS, spread over an energy range of $k_B T_g$. The density of TS in energy should therefore decrease as $1/T_g$ in approximate agreement with experiment.

7.4. Suffix

The ideas presented in §§ 2–6 have been very successful in understanding and relating a wide range of low-temperature physical phenomena in glasses on the basis of a general tunnelling state model. The general features of this model follow from the basic properties of the amorphous or disordered state, namely a wide range of local environments in which atoms do not have well defined local minima. However, two basic questions remain: why is the number of tunnelling states comparable in all glass-forming systems, and what (in the absence of impurities) is the microscopic structure of a tunnelling state?

These two questions will not be answered in a single all-embracing theory. An answer to the first may follow from a refinement of the general considerations described in § 7.3, but also, on the experimental side, from correlations between low-temperature

and glass-forming properties (Hunklinger and Raychaudhuri 1986). It is worth emphasising that reasonably complete data is available only on a very limited number of materials, notably vitreous silica and As_2S_3.

A convincing microscopic description of a tunnelling state in any amorphous material remains a problem to tax the solid state physicist. The key word is 'convincing'. Any analysis requires careful justification of structure and interatomic force constants (bearing in mind the difficulty of handling long-range forces in the amorphous state), related through the relaxation of the structure. Furthermore, there is no well defined procedure for calculating energy barriers between atomic configurations, although the technique of searching for low-frequency local vibrational states may provide a way forward (Guttman and Rahmann 1985).

Acknowledgments

I would like to thank Karin Arnold and Keith Papworth for invaluable help in the preparation of the manuscript.

References

Abramowitz M and Stegun I A 1970 *Handbook of Mathematical Functions* (New York: Dover)
Ackerman D A, Moy D, Potter R C, Anderson A C and Lawless W N 1981 *Phys. Rev.* B **23** 3886
Anderson A C 1986 *Phys. Rev.* B **34** 1317
Anderson P W 1975 *Phys. Rev. Lett.* **34** 953
Anderson P W, Halperin B I and Varma C M 1972 *Phil. Mag.* **25** 1
Araki H, Park G, Hikata A and Elbaum C 1980 *Phys. Rev.* B **21** 4470
Arnold W, Doussineau P, Frénois C and Levelut A 1981 *J. Physique Lett.* **42** L289
Arnold W, Doussineau P and Levelut A 1982 *J. Physique Lett.* **43** L695
Arnold W, Martinon C and Hunklinger S 1978 *J. Physique Colloq.* **39** C6 961
Barron T H K 1965 *Lattice Dynamics* ed R F Wallis (Oxford: Pergamon) p 247
Bernard L, Piché L, Schumacher G and Joffrin L J 1978 *J. Physique Colloq.* **39** C6 957
—— 1979 *J. Low Temp. Phys.* **35** 411
Black J L 1978 *Phys. Rev.* B **17** 2740
—— 1981 *Glassy Metals I* (*Topics in Applied Physics* **46**) ed H J Güntherodt and H Beck (Berlin: Springer) p 167
Black J L and Fulde P 1979 *Phys. Rev. Lett.* **43** 453
Black J L, Gyorffy B L and Jäckle J 1979 *Phil. Mag.* B **40** 331
Black J L and Halperin B I 1977 *Phys. Rev.* B **16** 2879
Brawer S A 1981 *Phys. Rev. Lett.* **46** 778
Buchenau U, Nücker N and Dianoux A J 1984 *Phys. Rev. Lett.* **53** 2316
Buchenau U, Prager M, Nücker N, Dianoux A J, Ahmad N and Phillips W A 1986 *Phys. Rev.* B **34** 5665
Cohen M H and Grest G S 1980 *Phys. Rev. Lett.* **45** 1271
—— 1981 *Solid State Commun.* **39** 143
Continento M A 1982 *Phys. Rev.* B **25** 7820
Cordié P and Bellessa G 1981 *Phys. Rev. Lett.* **47** 106
Duffy D M and Rivier N 1983 *Physica* **108B** 1261
Duquesne J Y and Bellessa G 1983 *J. Phys. C: Solid State Phys.* **16** L65
—— 1985 *Phil. Mag.* B **52** 821
Elliott S R 1979 *Phil. Mag.* B **40** 507
Esquinazi P, Ritter H M, Neckel H, Weiss G and Hunklinger S 1986 *Z. Phys.* B **64** 81
Etherington G, Wright A C, Wenzel J T, Dore J C, Clarke J H and Sinclair R N 1982 *J. Non-Cryst. Solids* **48** 265
Fox D L, Golding B and Haemmerle W H 1982 *Phys. Rev. Lett.* **49** 1356
Frossatti G, Gilchrist J le G, Lasjaunias J C and Meyer W 1977 *J. Phys. C: Solid State Phys.* **10** L515

Golding B and Graebner J E 1981 *Amorphous Solids: Low Temperature Properties* (*Topics in Current Physics* **24**) ed W A Phillips (Berlin: Springer)
Golding B, Graebner J E, Halperin B and Schutz R J 1973 *Phys. Rev. Lett.* **30** 223
Golding B, Graebner J E and Kane A B 1976a *Phys. Rev. Lett.* **37** 1248
Golding B, Graebner J E, Kane A B and Black J L 1978 *Phys. Rev. Lett.* **41** 1487
Golding B, Graebner J E and Schutz R J 1976b *Phys. Rev.* B **14** 1660
Golding B, Schickfus M v, Hunklinger S and Dransfeld K 1979 *Phys. Rev. Lett.* **43** 1817
Goubau W M and Tait R A 1975 *Phys. Rev. Lett.* **34** 1220
Graebner J E and Allen L C 1984 *Phys. Rev.* B **29** 5626
Graebner J E, Allen L C, Golding B and Kane A B 1983 *Phys. Rev.* B **27** 3697
Graebner J E and Golding B 1979 *Phys. Rev.* B **19** 964
Guttman L and Rahman S M 1985 *Phys. Rev.* B **33** 1506
Hagarty J, Broer M M, Golding B, Simpson J R and MacChesney J B 1982 *Phys. Rev. Lett.* **51** 2033
Hikata A, Cibuzar G and Elbaum C 1981 *J. Low Temp. Phys.* **49** 341
Hu P and Walker L R 1977 *Solid State Commun.* **24** 813
Huber D L, Broer M M and Golding B 1984 *Phys. Rev. Lett.* **52** 2281
Hui J C K and Allen P B 1975 *J. Phys. C: Solid State Phys.* **8** 2923
Hunklinger S and Arnold W 1976 *Physical Acoustics* vol XII, ed W P Mason and R N Thurston (New York: Academic) p 153
Hunklinger S, Arnold W, Stein S, Nava R and Dransfeld K 1972 *Phys. Lett.* A **42** 253
Hunklinger S and Raychaudhuri A K 1986 *Prog. Low Temp. Phys.* vol. IX, ed D F Brewer (Amsterdam: Elsevier) p 265
Hunklinger S and Schmidt M 1984 *Z. Phys.* B **54** 93
Isnard R and Gilchrist J le G 1981 *Chem. Phys.* **52** 111
Jäckle J, Piché L, Arnold W and Hunklinger S 1976 *J. Non-Cryst. Solids* **20** 365
Jones D P 1982 *Thesis* University of Cambridge
Jones D P, Thomas N and Phillips W A 1978 *Phil. Mag.* B **38** 271
Karpov V G 1985 *Sov. Phys.-Semicond.* **19** 74
Karpov V G, Klinger M I and Ignat'ev F N 1983 *Sov. Phys.-JETP* **57** 439
Keating P N 1966 *Phys. Rev.* **145** 637
Klauder J R and Anderson P W 1962 *Phys. Rev.* **125** 912
Kummer R B, Dynes R C and Narayanamurti V 1978 *Phys. Rev. Lett.* **40** 1187
Laikhtman B D 1985 *Phys. Rev.* B **31** 490
Lasjaunias J C, Maynard R and Vandorpe M 1978 *J. Physique Colloq.* **39** C6 973
Lasjaunias J C, Ravex A, Vandorpe M and Hunklinger S 1975 *Solid State Commun.* **17** 1045
Landau L D and Lifshitz E M 1984 *Electrodynamics of Continuous Media* (Oxford: Pergamon) 2nd edn
Lewis E, Lasjaunias J C and Schumacher G 1978 *J. Physique Colloq.* **39** C6 967
Licciardello D C, Stein D L and Haldane F D M 1981 *Phil. Mag.* B **43** 189
Löhneysen H v 1981 *Phys. Rep.* **79** 161
Löhneysen H v and Schink H J 1982 *Phys. Rev. Lett.* **48** 1121
Long A R 1982 *Adv. Phys.* **31** 553
Loponen M T, Dynes R C, Narayanamurti V and Garno J P 1980 *Phys. Rev. Lett.* **45** 457
—— 1982 *Phys. Rev.* B **25** 4310
Lou L F 1976 *Solid State Commun.* **19** 335
Lyo S K 1982 *Phys. Rev. Lett.* **48** 688
Meissner M and Spitzmann K 1981 *Phys. Rev. Lett.* **46** 265
Mertzbacher E 1970 *Quantum Mechanics* (New York: Wiley) 2nd edn
Mon K K and Ashcroft N W 1977 *Solid State Commun.* **27** 609
Narayanamurti V and Pohl R O 1970 *Rev. Mod. Phys.* **42** 201
Pelous J and Vacher R 1976 *Solid State Commun.* **19** 627
Phillips J C 1979 *J. Non-Cryst. Solids* **34** 153
—— 1981a *Phys. Rev.* B **24** 1744
Phillips W A 1972 *J. Low Temp. Phys.* **7** 351
—— 1973 *J. Low Temp. Phys.* **11** 757
—— 1976 *Phil. Mag.* **34** 983
—— 1981b *Amorphous Solids: Low Temperature Properties* (*Topics in Current Physics* **24**) (Berlin: Springer)
—— 1981c *Phil. Mag.* B **43** 747
—— 1985a *Physics of Disordered Materials* ed D Adler, H Fritzche and S R Ovshinsky (New York: Plenum) p 1329
—— 1985b *J. Non-Cryst. Solids* **77-78** 1329

Pippard A B 1983 *The Physics of Vibrations* vol 2 (Cambridge: Cambridge University Press)
Pohl R O, Love W F and Stephens R B 1974 *Proc. 5th Int. Conf. on Amorphous and Liquid Semiconductors* ed J Stuke and W Brenig (London: Taylor and Francis) p 1121
Raychaudhuri A K and Hunklinger S 1984 *Z. Phys.* B **57** 113
Redfield D 1971 *Phys. Rev. Lett.* **27** 730
Rothenfusser M, Dietsche W and Kinder H 1983 *Phys. Rev.* B **27** 5196
Russo G and Ferrari L 1984 *Phil. Mag.* B **49** 311
Sargent M, Scully M O and Lamb W E 1974 *Laser Physics* (Reading, MA: Addison-Wesley)
Schickfus M v and Hunklinger S 1976 *J. Phys. C: Solid State Phys.* **9** L439
—— 1977 *Phys. Lett.* **64A** 144
Slichter C P 1980 *Principles of Magnetic Resonance* (Berlin: Springer)
Smith D A 1978 *Phys. Rev. Lett.* **42** 729
Stephens R B 1973 *Phys. Rev.* B **8** 2896
Street R A and Mott N F 1976 *Phys. Rev. Lett.* **35** 1293
Thijssen H P H, Dicker A I M and Völker S 1982 *Chem. Phys. Lett.* **92** 7
Thomas N 1983 *Phil. Mag.* B **48** 297
Thorpe M F 1983 *J. Non-Cryst. Solids* **57** 355
Vacher R and Pelous J 1976 *Phys. Rev.* B **14** 823
Vukcevich M R 1972 *J. Non-Cryst. Solids* **11** 25
Wooten F and Weaire D 1984 *J. Non-Cryst. Solids* **64** 325
Wright O B 1986 *Phil. Mag.* B **53** 477
Wright O B and Phillips W A 1984 *Phil. Mag.* **50** 63
Zaitlin M P and Anderson A C 1975 *Phys. Rev.* B **12** 4475
Zeller R C and Pohl R O 1971 *Phys. Rev.* B **4** 2029
Zimmerman J and Weber G 1981 *Phys. Rev. Lett.* **46** 661